# Decoupled diversity and disparity after faunistic turnover in caviomorph rodents

Juan D. Carrillo*[1,2], María F. Torres Jiménez[3], Francisco J. Urrea-Barreto[4,5], Alexandre Antonelli[2,6,7,8], Christine Bacon[2], Søren Faurby[2], Daniele Silvestro[1,2]

1. Department of Biology, University of Fribourg, and Swiss Institute of Bioinformatics, Fribourg, CH1700, Switzerland.
2. Department of Biological and Environmental Sciences, and Gothenburg Global Biodiversity Centre, University of Gothenburg, Box 461, SE 405 30 Gothenburg, Sweden.
3. Institute of Biosciences, Life Sciences Center, Vilnius University, Vilnius, Lithuania.
4. Consejo Nacional de Investigaciones Científicas y Técnicas (CONICET), Museo Paleontológico Egidio Feruglio, Trelew, U9100GYO, Argentina.
5. Smithsonian Tropical Research Institute, 0843-03092 Balboa, Panama.
6. Royal Botanic Gardens, Kew, Richmond, Surrey, TW9 3AE, UK.
7. Wuhan Botanic Garden, Chinese Academy of Sciences, Wuhan, China.
8. Department of Biology, University of Oxford South Parks Road, Oxford, OX1 3RB, UK.

***Corresponding author:** Juan D. Carrillo
Chemin du Musée 10, Fribourg, CH1700, Switzerland.
**Email:** juan.carrillo@unifr.ch

**Author Contributions:** J.D.C. and D.S. designed the research; J.D.C., M.F.T.J., and D.S. performed the research; J.D.C., M.F.T.J., F.J.U-B., D.S. contributed analytic tools; J.D.C., M.F.T.J., F.J.U-B., A.A., C.B., S.F., and D.S. analyzed data and wrote the paper.

**Keywords:** Body mass; Diversification; Morphological evolution; Rodentia; South America.

## Abstract

Understanding the relationship between species diversity and morphological disparity in evolutionary radiations is a major challenge in macroevolution. Caviomorpha diversified in the Americas, and the sister clades Octodontoidea and Chinchilloidea (including spiny rats and chinchillas, respectively) provide a striking example of imbalanced evolution. These clades vary in diversity with 195 extant species in the former and six extant species in the latter. However, fossils document a higher past diversity and disparity in Chinchilloidea, including the largest rodents that ever existed. We combine data from extant and extinct species to evaluate how evolutionary dynamics shaped their contrasting diversity and disparity patterns. We inferred a phylogeny including 149 extant and 52 extinct species, and used craniodental traits and body mass to infer morphological evolution. Our results indicate that the most recent common ancestor of Chinchilloidea and Octodontoidea lived during the late Eocene (~36.5 Ma). The inferred ancestral body mass was small (~187 gr), but grew in range over time in Chinchilloidea. Although rates of morphological evolution in Chinchilloidea were significantly higher than in Octodontoidea, these clades shared similar diversity trajectories until an Oligocene turnover event. Octodontoidea then began increasing diversity until the present, whereas Chinchilloidea diversity stagnated and dropped in the late Miocene and Pleistocene. Neogene and Quaternary extinctions in Chinchilloidea reversed a pattern of relative higher disparity than Octodontoidea that had lasted for ~30 million years. We show a case of remarkable decoupling between diversity and disparity, highlighting complex relationships between ecomorphology, species richness, and how they were affected by extinctions.


## Significance Statement

Caviomorpha includes two closely related rodent groups that diversified in South America. Octodontoidea and Chinchilloidea (including spiny rats and chinchillas, respectively). Although Octodontoidea species diversity is 32-fold higher than Chinchilloidea, fossils document higher past diversity and morphological variation in the latter, including the largest rodents that ever lived. We combined data from extinct and living species and used phylogenetic comparative methods to study their diversity and morphology evolutionary dynamics. We found higher rates of morphological evolution in Chinchilloidea. The groups show similar diversity until an Oligocene turnover event. Subsequently, Octodontoidea diversity was higher. Recent extinctions reversed a long-term pattern of higher morphological variation in Chinchilloidea. These results show how complex interactions shape the diversity and morphological evolution in evolutionary radiations.

## Main Text

### Introduction

Understanding the relation between species diversification and morphological variation (hereafter disparity) in evolutionary radiations is a major challenge in macroevolution and paleobiology (1, 2). Eco-evolutionary models make predictions on the relationship between species richness (hereafter diversity) and disparity. In adaptive radiations, a rapid diversification is accompanied by ecological and morphological differentiation (3, 4), whereas in non-adaptive radiations clades diversify with minimal ecological and morphological differentiation (5, 6). Studies on a range of different taxa have yielded contrasting results, with some finding patterns of diversity and disparity in evolutionary radiations to be coupled (e.g., 7, 8) and others finding them to be decoupled (e.g., 9–11).

Incorporating fossil information to the study of biological radiations is key, as they document diversification dynamics and morphological evolution in deep time. The fossil record has served to clarify the relationship between diversity and disparity in evolutionary radiations of several clades, also finding contrasting results of coupling and decoupling on different taxa (e.g., 10, 12–

14). While studies of major radiations of different clades and geographic regions are required to elucidate the general patterns of diversity and disparity dynamics, a powerful opportunity is to test the evolutionary patterns in sister clades that radiated in the same geographic region and may help reveal the underlying evolutionary processes, by removing many confounding effects such as different evolutionary pressures in different regions.

Sister clades can show striking imbalances in diversity (15, 16). Empirical phylogenetic trees are more imbalanced than predicted by simple macroevolutionary models (16, 17). Simulations and empirical data suggest that tree imbalance can be driven by differences in age-dependent speciation, stochastic population-level processes, and the appearance of key innovations (17–20), among other potential causes. Sister clades may also follow different patterns of morphological evolution (21).

One clade that could help illuminate the relationship between diversity and disparity is the Caviomorpha. This highly diverse clade of rodents is endemic to the Americas, including the Caribbean islands. It has a rich fossil record that is informative of the major pathways of its evolution (22). Caviomorphs are recorded in the fossil record in South America since at least the late Eocene–early Oligocene (~36 – 30 Ma), and presumably arrived to the continent through rafting from Africa (23–25). Subsequently, caviomorphs radiated throughout South America and by the late Oligocene (~27–23 Ma) they were highly diverse, with representatives of the main extant clades already evolved (22, 25, 26). The caviomorph radiation is therefore a suitable system to study patterns and processes of diversification and morphological evolution thanks to their rich fossil record, high taxonomic and ecological diversity, and phenotypic disparity (22, 27–30).

Extant caviomorphs are grouped in four clades which are well supported by molecular and morphological data: Caviodea, Chinchilloidea, Erethizontoidea, and Octodontoidea (26, 28, 31, 32). The Octodontoidea (spiny rats, tuco-tucos, degus, hutias, and related species) and Chinchilloidea (chinchillas, pacaranas, and their related species) are sister clades, which diverged early in the caviomorph radiation (22, 26, 28, 32, 33). The abundant fossil record of Octodontoidea documents its evolution and past diversity (e.g., 34–38). Octodontoidea is highly diverse today, including 195 extant species, and it is widely distributed in the Americas and the Caribbean islands (30, 33, 39–41). The clade includes arboreal, burrowing, terrestrial, and semiaquatic forms with different diets (29). The Octodontoidea exhibit important morphological variation (36, 42, 43), and includes large species such as the Capromyidae in the Caribbean islands (44, 45). However, the clade displays a narrower range of disparity (e.g., variation in body mass) in comparison with other caviomorph clades (28).

In contrast to the current high diversity in Octodontoidea, Chinchilloidea is represented today by only six species with most of its extant species found in the Andes (30, 40, 41). However, the fossil record documents a higher past diversity and morphological variation within the clade (e.g., 22, 46–52). Fossil Chinchilloidea also have remarkable disparities, including species that reached giant sizes, with body mass estimates of about 150 to 500 kg (*Phoberomys pattersoni*, *Josephartiasia monesi* 53–56), while a chinchilla weighs about 400 gr. Chinchilloidea also includes the Heptaxodontidae, a group of large extinct caviomorphs recorded during the Quaternary in the Caribbean islands (26, 57–60) (but see [58, 60] on alternative hypotheses of the relationships of *Elamodostomys*).

Here, we study the dynamics of diversity and disparity that led to the diversity imbalance of sister clades in caviomorphs. We combine data from extant and extinct species of Octodontoidea and

Chinchilloidea to evaluate how their diversification dynamics led to the current imbalance in species diversity and morphological evolution.

## Results

We performed a time-calibrated phylogenetic analysis for living and fossil Octodontoidea and Chinchilloidea using molecular and morphological data. The inferred relationships among extant species are well supported (bootstrap node support of the families and main clades >0.90; Figs. S1-S2) and consistent with previous studies regarding the interrelationships of extant clades (e.g., 32, 39). The total evidence phylogenetic analysis indicates an early Oligocene origin for crown Octodontoidea and Chinchilloidea, with an age of origin of 31.6 Ma (CI = 28.7 – 35.8 Ma) for crown Octodontoidea and 32.4 Ma (CI = 30.1 – 35.2 Ma) for crown Chinchilloidea (Fig. S3). The age of the Octodontoidea + Chinchilloidea obtained from an independent analysis of the fossil record using a Bayesian Brownian bridge model (61) indicated a late Eocene origin, with a mean of 36.5 Ma (95% credible interval [CI] = 33.0 – 40.8 Ma) (Fig. S4).

We determined disparity through time, by analyzing the evolution of body mass of extinct and extant Octodontoidea and Chinchilloidea using phylogenetic comparative methods. The ancestral body mass of Chinchilloidea + Octodontoidea was small, with a mean estimate of ~187 gr (CI = 120 – 305 gr). The two clades had similarly small body mass at their origin but subsequently Chinchilloidea showed a higher body mass range through time (Fig.1A, D), it reached the highest body mass values in the Pliocene and Pleistocene (5.3 – 0.012 Ma) and decreased towards the present (Fig. 1A, D; S5A). In contrast, Octodontoidea body mass remained relatively stable throughout the Paleogene and Neogene, reaching its largest body mass range at the present (Fig. 1; S5).

The estimated rate of body mass evolution was about 4.3 times higher in Chinchilloidea compared with Octodontoidea (Fig. 1B; S5B). We found support for a positive trend towards higher body mass in Chinchilloidea (posterior probability: 0.93), but did not find evidence for a trend in Octodontoidea (Fig. 1C, Table 2). These results and overall patterns in body mass evolution where consistently inferred even under models without a trend parameter (Figs. 1; S5).

We estimated diversity trajectories and net diversification rates of Chinchilloidea and Octodontoidea to identify how and when the diversity imbalance unfolded. We used lineage through time plots to quantify the diversity dynamics of the two clades. The diversity trajectories of Chinchilloidea and Octodontoidea were similar during the Paleogene. The diversity of both clades increased since their origin until the early Oligocene (~30 Ma), when a decrease in species diversity is observed in both clades (Fig. 2A). Subsequently, Octodontoidea showed a trend of increasing diversity, which continues until the present, whereas Chinchilloidea diversity stagnated, and showed two periods of diversity decrease, during the late Miocene and in the Pleistocene (Fig. 2A).

We inferred the diversification dynamics by estimating the rates net diversification (origination minus extinction) for each clade under a piecewise-constant fossilized birth death process (62). The diversification dynamics of Chinchilloidea and Octodontoidea were similar during the Paleogene and differed in the late Miocene and Quaternary (Fig. 2B). The diversification rates of both clades were high in the Eocene (0.28 [CI= -0.08 – 0.74] for Octodontoidea and 0.31 [CI = -0.01 – 0.69] for Chinchilloidea) and decreased in the Oligocene to 0.04 [CI= -0.12 – 0.21] in Octodontoidea and -0.01 [CI = -0.16 – 0.14] in Chinchilloidea. Octodontoidea showed higher diversification rates than Chinchilloidea during the late Miocene (0.12 [CI=-0.04 – 0.28] vs. -0.24

[CI = -0.60 – 0.10]) and the difference further increased in the Quaternary (3.45 [CI= 2.86 – 4.13] for Octodontoidea and 1.97 [CI = 0.72 – 3.49] for Chinchilloidea) (Fig. 2B).

We inferred morphospace occupation using body mass and cranial trait data of living species of the two clades (Fig. 3). Although extant Octodontoidea occupied a larger area of the morphospace than Chinchilloidea, when we accounted for the differences in species diversity through random subsampling, the morphospace occupancy of Chinchilloidea was not statistically different from that of Octodontoidea (Fig. 3B-C). Despite the differences in current species diversity between Chinchilloidea and Octodontoidea, the former clade occupies a considerable portion of the cranial morphospace in comparison with the latter (Fig. 3).

## Discussion

We evaluated the relationship between diversity and disparity between two major sister clades (Octodontoidea and Chinchilloidea) of caviomorphs that radiated in South America, combining data from extinct and extant species. We found higher rates of morphological evolution in Chinchilloidea, whereas Octodontoidea showed higher diversification rates that led to the current imbalance in species diversity between the two clades. Despite having a higher disparity, Chinchilloidea showed a lower diversity than Octodontoidea during most of their evolutionary time. Late Neogene and Quaternary extinctions in Chinchilloidea disproportionally reduced its morphological disparity.

### Diversification dynamics

Our results indicate that the clade Octodontoidea + Chinchilloidea originated in the late Eocene (~36.5 Ma), shortly after the arrival of caviomorphs to South America. The oldest fossil records of caviomorphs on the continent are at least early Oligocene in age (25), but possibly as old as the Eocene-Oligocene transition (23, 24). Fossils provide a minimum age, and our estimates of late Eocene origin of Octodontoidea + Chinchilloidea are in agreement with recent estimates of middle Eocene origin of crown Caviomorpha (25). The diversity curves and diversification rates were similar for Octodontoidea and Chinchilloidea during the Paleogene (Fig. 2). The lineage through time plot showed that the diversity of both clades decreased in the early Oligocene, which likely reflects a faunistic turnover event in the mammalian fauna of South America known as the Patagonian Hinge and driven by global cooling (63).

The stark difference in species diversity of extant Octodontoidea and Chinchilloidea is the result of contrasting diversification dynamics during the Neogene (Fig. 2). Since the second half of the Oligocene, Octodontoidea diversity increased until the beginning of the Miocene, which corresponds to a diversification pulse of lineages in southern South America (38). Subsequently, Octodontoidea diversity steadily increased from the middle Miocene to the present (Fig. 2A), with the appearance of several modern lineages in the late Miocene (38). Octodontoidea showed two time periods with higher diversification rates compared to its sister clade, the late Miocene and the Quaternary (Fig. 2B). The higher diversification rates of Octodontoidea are possibly associated with important environmental changes and geologic events in South America, such as the central and northern Andean uplift during the Neogene (64, 65). The spiny rats (Echimyidae, Octodontoidea) experienced dispersal and vicariant events among different biogeographic regions which impacted the diversification of the group (39, 66, 67).

The higher diversification of Octodontoidea could be also related to dispersal and subsequent diversification in other continental regions during the Neogene. The clade has a wide geographical distribution, including lineages that colonized tropical Central America (Echimyidae) (33), as part of the Great American Biotic Interchange (68). Biogeographical studies based on molecular data estimate that the hutias (Capromyidae, Octodontoidea) dispersed to the Caribbean islands during the early to middle Miocene (39, 59), likely spurring additional diversification.

The fossil record documents a higher diversity of Chinchilloidea in the past compared with their modern diversity of six species (22, 52). The lineage through time plot indicated that the species diversity of the clade remained relatively low during most of the Neogene and Quaternary (Fig 2A). After the diversity dropped in the early Oligocene, the Chinchilloidea diversity stagnated and remained low in comparison to Octodontoidea (Fig. 2A). The low diversification rates of Chinchilloidea during the late Miocene reflects the extinction of lineages that reached gigantic sizes within Dinomyidae and Neoepiblemidae (52, 56). Neoepiblemidae is an extinct clade of giant caviomorphs that has a rich fossil record in tropical South America (46, 69). Based on sedimentary and morphological features, it has been proposed that at least some neoepiblemid taxa (e.g., *Phoberomys*) were semi-aquatic (53, 55, 70). The drivers of the Neoepiblemidae extinction are not fully understood, but it is possible that landscape changes related with the evolution of the Amazonian drainage system during the late Neogene (71–73) contributed to the extinction of tropical neoepiblemids. The uplift of the central and northern Andes and the associated climatic and hydrographic changes in tropical South America have been associated with extinctions of aquatic vertebrates, such as crocodiles (74, 75). Additional extinctions of giant Chinchilloidea lineages occurred in the Quaternary, with the extinction of the giant hutias in the Caribbean islands, possibly caused by humans (26, 57, 58, 76). As result of the late Neogene and Quaternary extinctions, Chinchilloidea is today a species-poor clade, with only one known species present in the Amazon (the pacarana) and five species restricted to the Andes (30).

**Morphological evolution**

The analysis of body mass evolution showed that the ancestral body mass of Octodontoidea + Chinchilloidea was small (~187 gr). Subsequently, Chinchilloidea evolved a high range of body mass in comparison with Octodontoidea, with a trend of increasing size, and some lineages reached giant sizes during the late Neogene and Quaternary (Fig. 1). Extant caviomorphs are characterized by large body mass ranges and high rates of morphological evolution (28). Chinchilloidea is not the only caviomorph subclade that reached large size. The subclade Cavioidea also shows high rates of body mass evolution and includes the largest living rodent, the capybara which can weigh ~50 kg (22, 28).

Body mass increase in mammals is related to niche expansion, ecological specialization, and reduced competition (14, 77), among other possible factors. The evolution of large caviomorphs (>40 kg, subclades Chinchilloidea and Cavioidea) from the late Miocene to Quaternary could have resulted from a niche expansion related to new environmental and climatic conditions where some of these species lineages were found (e.g., expansion of open environments and drier climate in southern South America) (22, 28). An increase in herbivore body mass is related with a capacity to feed on a higher variety of plant parts and a decrease in diet quality (78). Chinchilloidea large to giant sizes were also reached by the Caribbean giant hutias, representing an outstanding case of insular gigantism (57).

The high Octodontoidea diversity is the result of steady diversification since the Miocene (Fig. 2). However, the increase in diversity was not accompanied by high morphological differentiation, in comparison with Chinchilloidea (Fig. 1). Within Octodontoidea, the tuco-tucos (*Ctenomys,* Ctenomyidae) have the highest rates of taxonomic diversification (28). Ctenomyidae is highly diverse (68 living species [41]), representing 35% of the current Octodontoidea diversity. The *Ctenomys* radiation occurred since the late Miocene-early Pliocene (Fig. S4) (28, 33, 38). Extant *Ctenomys* have subterranean habits, and occur in well-drained habitats in lowland and montane habitats of southern South America (79). Several living *Ctenomys* species have disjunct distributions and molecular data indicates a rapid and early diversification in the *Ctenomys* radiaton (79, 80). Rapid diversification is also observed on pocket gophers (Geomyidae) another group of fossorial rodents (81). A scenario of rapid diversification with little overlapping distribution might explain the high diversification with little morphological modification.

Chinchilloidea showed a high disparity and relative low diversity since early in its evolutionary history (Figs 1-2), but the late Neogene and Quaternary extinctions drastically reduced the disparity of the clade (Fig 1D). As result, extant Chinchilloidea shows a much lower disparity today, to the point that Chinchilloidea and Octodontoidea have comparable disparity when we account for differences in species diversity (Fig. 3). Thus, the recent extinctions had a disproportionate effect on the disparity of Chinchilloidea, reversing a pattern of relative higher disparity in comparison with Octodontoidea that appeared early in their origin (Fig. 1D).

The reason why the large disparity of Chinchilloidea was not accompanied with high species diversity might be linked to the propensity of the clade to evolve large body sizes. In living mammals, there seems to be a negative relationship between species diversity and body size (82, 83). The relative low diversity of large-bodied mammals could also be related to having lower larger range sizes, population sizes, longer generation times, and/or reduced reproductive output (18, 84–86).

Taken together, our results revealed contrasting patterns of diversity and disparity evolution for the sister clades Octodontoidea and Chinchilloidea. Extant Octodontoidea species diversity is 32-fold higher than the extant Chinchilloidea diversity. The differences in diversity started in the Miocene, and are due to higher diversification rates of Octodontoidea in the late Miocene and Quaternary. In contrast, Chinchilloidea shows higher disparity during the Neogene and Quaternary, including species that reached gigantic sizes. However, post-Pliocene extinctions in Chinchilloidea led to a drop in disparity in the group and extant Chinchilloidea today occupy a comparable morphospace area than Octodontoidea.

## Conclusion

An imbalance of species diversity between sister clades is common across the tree of life. An examination of the relationship between diversity imbalance and morphological evolution can shed light on the mechanisms underlying the relationship between taxonomic and morphological diversity. Our results indicate that sister groups that evolved in the same region and experienced similar environmental changes and ecological interactions, exhibit drastically different diversification and morphological evolution dynamics. Diversity and disparity patterns are ultimately also shaped by extinctions, which we showed can disproportionally reduce the disparity of a clade, reversing patterns of morphological evolution that had persisted for millions of years.

## Materials and Methods

*Phylogenetic analyses*

*Sequence retrieval and molecular alignment construction*

We retrieved all nucleotide sequences available in GenBank for the Caviomorpha subclades Chinchilloidea and Octodontoidea using the R libraries restez v1.0.2 (87) as implemented within supersmartR (88), and querying the NCBI taxIDs of genera belonging to those subclades (Table S2; accessed in April 2022). Sequences were grouped into locus clusters using phylotaR v.1.2.0 (88) and BLAST (89), with the minimum number of species in each cluster set to five and a minimum MAD score – a measure of sequence length disparity – of 0.4 (90). Taxonomic names below the species level (e.g., subspecies) were excluded. Each cluster was aligned using MAFFT (91), its identity corroborated against all vertebrate sequences using BLAST (89), and its gaps removed using ClipKIT (92) with the kpic-smart-gap model. We concatenated the resulting 49 clusters into two matrices (one mitochondrial and one nuclear) using python (Dataset S3). We used PartitionFinder2 (93) to find the best substitution and partition model for our data (Table S3), using the Greedy Algorithm and RAxML (94, 95), branch lengths linked, and the Akaike Information Criterion (AICc). The molecular alignment included 149 caviomorphs species, six species representing Chinchilloidea, and 143 species representing Octodontoidea.

*Time-calibrated phylogenetic analysis*

We undertook a total evidence phylogenetic analyses by combining the molecular alignment with a morphological matrix of extinct and extant caviomorphs based on Marivaux *et al.* (2020). For the morphological matrix, we included the Chinchilloidea and Octodontoidea species scored in the matrix of Marivaux *et al.* (2020), plus the closely related *Mayomys* and *Eosallamys.* In addition, because of their relevance to analyses of trait evolution, we included the extinct species *Phoberomys pattersoni* and *Josephartigasia monesi* that represent the largest body mass reached within Rodentia (53, 54, 56). As *Phoberomys* and *Josephartigasia* were not included in the original character matrix of Marivaux *et al.* (2020), for the phylogenetic analysis, we set taxonomical constraints for *Phoberomys* (constrained within Neoepiblemidae; Rasia *et al.* 2021) and *Josephartigasia* (constrained within Dinomyidae; Rinderknecht & Blanco 2008). The morphological matrix used in our phylogenetic analysis had 513 morphological characters, and included 64 species, 52 extinct and 12 extant.

We used the Bayesian Brownian bridge (BBB) model (61) to estimate the age of origin of the Octodontoidea + Chinchilloidea clade. The BBB model infers the age of origin of a clade based on its present diversity and fossil record (61). We obtained the extant diversity of Octodontoidea and Chinchilloidea (201 extant species) from the Mammal Diversity Database v.1.8 (40, 41). For the fossil taxa, we compiled from the literature the age ranges of the species of Octodontoidea and Chinchilloidea included in our study (Table S4). Then, we generated 100 replicates of the fossil species ages. For each replicate, we generated a random age for each fossil species drawn from a uniform distribution between its maximum and minimum age (Table S4). Finally, for each replicate we counted the number of species per 1 Ma time bins. After running the BBB analysis, we fit a gamma distribution to the estimates of age of origin for each replicate, which was used to set the prior of the age of origin (Fig. S4).

We conducted a Bayesian time-calibrated phylogenetic analysis combining the molecular and morphological matrices using BEAST2 v.2.6.7 (Bouckaert *et al.* 2019). The combined matrix includes 201 species (149 extant and 52 extinct). For time calibration, we used the oldest (maximum age within the age range) of each extinct species (Table S4). We used the Fossilized Birth-Death model (97) that models diversification and fossil sampling, and estimates phylogenetic relationships and divergence times within a single framework. We used one partition for the molecular data using the GTR + gamma model. The Lewis Mk model was used for the morphological partition (98). For the age of origin of Octodontoidea + Chinchilloidea clade, we used the gamma distribution fitted after the BBB analysis (shape = 4.68, rate = 1.043), and an offset of 32 Ma, the minimum observed origin age in our dataset (Table S4).

We used 1,000,000,000 iterations, sampling every 10,000. We used four chains (three heated, one cold) with a delta temperature of 0.03, and the coupled Markov Chain Monte Carlo (MCMC) algorithm (99). We used Tracer (100) for visualization and diagnostics of the MCMC output, and when summarizing the results, we discarded the first 60% of the samples as burn-in.

*Trait data*

We took 23 cranial measurements following Wilson (2013) and Tavares *et al.* (2016, 2018) (Fig. 3; Table S1). We measured 38 extant species, representing 28 of the 42 extant genera, and all families of Chinchilloidea and Octodontoidea (32). We measured a total of 220 specimens (Dataset S1), with a caliper to the nearest 0.01 mm. We measured specimens with erupted molars and low dental wear, scored with individual dental ages (IDAS) 3 or 4 (adult or late adult, respectively) following Anders *et al.* (2011). When possible, we measured up to ten specimens of the same species and used the average values in our analyses (Datasets S1-S2).

We compiled trait data for the extinct and extant caviomorph species included in our analyses. Body mass of extant species was compiled from the Phylacine database v.1.2.1 (103, 104), Patton *et al.* (2015) for *Ctenomys ibicuiensis*, and Emmons & Fabre (2018) for *Toromys*

*albiventris*. Body mass estimates of extinct species were compiled from the literature (Table S5). For extinct species without previously reported body mass, dental measurements were taken from literature to estimate their body mass using the regression equations provided by Millien & Bovy (2010) (Table S6). We used dental measurements because most fossil specimens consist of dental remains, and dental dimensions have been suggested as reliable proxies for body mass estimates in rodents (107).

*Trait evolution analyses*

We analyzed body mass evolution in a phylogenetic framework using Bayesian inference as implemented in the fossilBM program (108, 109). The fossilBM algorithm jointly estimates the rate and trend of trait evolution and the ancestral states for all internal nodes. The rate and trend parameters can vary among clades (108) and as a function of time (109). We used the fossilized Brownian motion model with and without trend, to evaluate the presence of positive or negative trends in the evolution of body mass.

To account for the uncertainty on body mass estimates from fossils, we generated 100 replicates with a random body mass for each extinct species derived from a normal distribution with parameters given by the mean body mass estimate and a standard deviation calculated from the body mass range (maximum and minimum estimates; Appendix 3). For each model (with and without trend), we ran the analyses for 5,000,000 MCMC iterations sampling every 5,000 and excluded the first 10% of the samples as burn-in. The analyses were run over a sample of 100 phylogenetic trees to account for topological and dating uncertainties. We summarized the rate and trend parameters and the inferred ancestral states by calculating the mean and 95% credible intervals after combining the output of the 100 replicates.

*Diversity and diversification analyses*

We constructed lineage through time (LTT) plots for Octodontoidea and Chinchilloidea. We estimated the number of lineages through time using the ape package v.5.7.1 (110) for the same 100 phylogenetic trees used for the analyses of trait evolution. We calculate the mean and 95% credible intervals of the number of lineages through time for each clade.

To evaluate diversification dynamics through time, we estimated the net diversification (origination minus extinction) using the Fossilized Birth-Death (FBD) skyline model (62, 111) as implemented in BEAST2 v.2.6.7 (96) and following (112). The FBD skyline model jointly estimates piecewise constant evolutionary rates and fossil sampling from phylogenies. We estimated diversification rates for each clade using the sample of 100 trees used in all analyses, for the following time bins: Eocene, Oligocene, early, middle and late Miocene, Pliocene, and Quaternary (Pleistocene and Holocene).

*Morphospace of extant Octodontoidea and Chinchilloidea*

We constructed a phylomorphospace (projection of a phylogenetic tree into a bivariate morphospace) using the phytools package (113). We used the trait data (23 cranial measurements and body mass) collected for the extant species of Octodontoidea and Chinchilloidea. We performed a principial components analysis (PCA) using the trait data with the FactoMineR package (114). Finally, we used the maximum credibility tree obtained from the total evidence analysis (Fig. S3) pruned to include only the 38 extant species with trait data and we constructed a phylomorphospace of the two principal components with phytools (113).

Extant Chinchilloidea is species poor (six species, five represented in our trait sample) in comparison with extant Octodontoidea (196 species, 33 represented in our trait sample) (40, 41). To account for differences in the number of extant species between the two clades, we resampled five Octodontoidea species at random from the trait dataset and calculate the area of the morphospace occupied (the area of the convex hull defined by those species). We resampled

100 times and calculate the frequency distribution and median of the morphospace area to compare with the area occupied by the five Chinchilloidea species.

*Data availability*

All the input and output files of the analyses described below, as well as the associated code are available in SwicthDrive https://drive.switch.ch/index.php/s/fULTN4t4Sqf2f1t.

**Acknowledgments**

We would like to acknowledge the following curators for access to the collections under their care: D. Kalthoff (Naturhistoriska riksmuseet, Stockholm), M. Gelang (Naturhistoriska Museum, Gothenburg), V. Nicolas and A. Verguin (Museum National d'Histoire Naturelle, Paris), M. Surovy (American Museum of Natural History, New York), D. Lunde (National Museum of Natural History, Washington), H. López (Instituto de Ciencias Naturales, Bogotá). JDC acknowledges support by the Swiss National Science Foundation grants P2ZHP3_174749, P4P4PB_199187, and TMPFP2_209818, and the Helge Ax:son Johnson Stiftelse grant F18-0486. AA acknowledges support from the Swedish Research Council (2019-05191) and the Kew Foundation. The Interfaculty Bioinformatics Unit (IBU), University of Bern provided computational infrastructure and support with bioinformatic analyses. We are grateful to R. Warnock and B. Allen for valuable comments.

**References**

1. M. Foote, A. I. Miller, *Principles of Paleontology*, 3rd Ed. (Freeman and Company, 2007).

2. M. J. Benton, Exploring macroevolution using modern and fossil data. *Proceedings of Royal Society of Biology* **282**, 20150569 (2015).

3. G. G. Simpson, *The Tempo and Mode in Evolution* (Columbia University Press, 1944).

4. D. Schluter, *The Ecology of Adaptive Radiation* (Oxford University Press, 2000).

5. E. Gittenberger, What about non-adaptive radiation? *Biological Journal of the Linnean Society* **43**, 263–272 (1991).

6. R. J. Rundell, T. D. Price, Adaptive radiation, nonadaptive radiation, ecological speciation and nonecological speciation. *Trends in Ecology & Evolution* **24**, 394–399 (2009).

7. L. J. Harmon, J. A. Schulte, A. Larson, J. B. Losos, Tempo and mode of evolutionary radiation in iguanian lizards. *Science* **301**, 961–964 (2003).

8. D. L. Rabosky, *et al.*, Rates of speciation and morphological evolution are correlated across the largest vertebrate radiation. *Nat Commun* **4**, 1958 (2013).

9. D. C. Adams, C. M. Berns, K. H. Kozak, J. J. Wiens, Are rates of species diversification correlated with rates of morphological evolution? *Proceedings of the Royal Society B: Biological Sciences* **276**, 2729–2738 (2009).

10. J. L. Cantalapiedra, J. L. Prado, M. Hernández Fernández, M. T. Alberdi, Decoupled ecomorphological evolution and diversification in Neogene-Quaternary horses. *Science* **355**, 627–630 (2017).

11. R. V. Missagia, D. M. Casali, B. D. Patterson, F. A. Perini, Decoupled Patterns of Diversity and Disparity Characterize an Ecologically Specialized Lineage of Neotropical Cricetids. *Evol Biol* (2023) https:/doi.org/10.1007/s11692-022-09596-8 (March 7, 2023).

12. R. B. J. Benson, *et al.*, Rates of dinosaur body mass evolution indicate 170 million years of sustained ecological innovation on the avian stem lineage. *PLoS Biology* **12**, e1001853 (2014).

13. A. Goswami, *et al.*, Attenuated evolution of mammals through the Cenozoic. *Science* **378**, 377–383 (2022).

14. O. Sanisidro, M. C. Mihlbachler, J. L. Cantalapiedra, A macroevolutionary pathway to megaherbivory. *Science* **380**, 616–618 (2023).

15. A. O. Mooers, S. B. Heard, Inferring evolutionary process from phylogenetic tree shape. *The Quarterly Review of Biology* **72**, 31–54 (1997).

16. L. F. Henao-Diaz, M. Pennell, The Major Features of Macroevolution. *Systematic Biology*, syad032 (2023).

17. O. Hagen, K. Hartmann, M. Steel, T. Stadler, Age-dependent speciation can explain the shape of empirical phylogenies. *Systematic Biology* **64**, 432–440 (2015).

18. L. Van Valen, Adaptive zones and the orders of mammals. *Evolution* **25**, 420–428 (1971).

19. J. P. Hunter, Key innovations and the ecology of macroevolution. *Trends in Ecology & Evolution* **13**, 31–36 (1998).

20. T. J. Davies, A. P. Allen, L. Borda-de-Água, J. Regetz, C. J. Melián, Neutral biodiversity theory can explain the imbalance of phylogenetic trees but not the tempo of their diversification. *Evolution* **65**, 1841–1850 (2011).

21. T. Blankers, T. M. Townsend, K. Pepe, T. W. Reeder, J. J. Wiens, Contrasting global-scale evolutionary radiations: phylogeny, diversification, and morphological evolution in the major clades of iguanian lizards. *Biological Journal of the Linnean Society* **108**, 127–143 (2013).

22. M. G. Vucetich, M. Arnal, C. M. Deschamps, M. E. Perez, E. C. Vieytes, “A Brief History of Caviomorph Rodents as Told by the Fossil Record” in *Biology of Caviomorph Rodents: Diversity and Evolution*, A. I. Vassallo, D. Antenucci, Eds. (SAREM- Sociedad Argentina para el Estudio de los Mamíferos, 2015), pp. 11–62.

23. P.-O. Antoine, *et al.*, Middle Eocene rodents from Peruvian Amazonia reveal the pattern and timing of caviomorph origins and biogeography. *Proceedings of the Royal Society B: Biological Sciences* **279**, 1319–1326 (2012).

24. P.-O. Antoine, *et al.*, Biotic community and landscape changes around the Eocene–Oligocene transition at Shapaja, Peruvian Amazonia: Regional or global drivers? *Global and Planetary Change* **202**, 103512 (2021).

25. K. E. Campbell, P. B. O’Sullivan, J. G. Fleagle, D. de Vries, E. R. Seiffert, An Early Oligocene age for the oldest known monkeys and rodents of South America. *Proc Natl Acad Sci USA* **118**, e2105956118 (2021).

26. L. Marivaux, *et al.*, Early Oligocene chinchilloid caviomorphs from Puerto Rico and the initial rodent colonization of the West Indies. *Proceedings of the Royal Society B* **287**, 20192806 (2020).

27. A. Álvarez, S. I. Perez, D. H. Verzi, Ecological and phylogenetic dimensions of cranial shape diversification in South American caviomorph rodents (Rodentia: Hystricomorpha). *Biological Journal of the Linnean Society* **110**, 898–913 (2013).

28. A. Álvarez, R. L. M. Arévalo, D. H. Verzi, Diversification patterns and size evolution in caviomorph rodents. *Biological Journal of the Linnean Society* **121**, 907–922 (2017).

29. R. A. Ojeda, A. Novillo, A. A. Ojeda, "Large-scale richness patterns, biogeography and ecological diversification in caviomorph rodents" in *Biology of Caviomorph Rodents: Diversity and Evolution*, (2015), pp. 121–138.

30. R. Maestri, B. D. Patterson, Patterns of species richness and turnover for the South American rodent fauna. *Plos One* **11**, e0151895 (2016).

31. P.-H. Fabre, L. Hautier, D. Dimitrov, P. Douzery, J. Emmanuel, A glimpse on the pattern of rodent diversification: a phylogenetic approach. *BMC evolutionary biology* **12**, 88 (2012).

32. N. S. Upham, B. D. Patterson, "Evolution of caviomorph rodents: a complete phylogeny and timetree for living genera" in *Biology of Caviomorph Rodents: Diversity and Evolution*, A. I. Vasallo, D. Antenucci, Eds. (SAREM- Sociedad Argentina para el Estudio de los Mamíferos, 2015), pp. 63–120.

33. N. S. Upham, B. D. Patterson, Diversification and biogeography of the Neotropical caviomorph lineage Octodontoidea (Rodentia: Hystricognathi). *Molecular Phylogenetics and Evolution* **63**, 417–429 (2012).

34. D. Verzi, A. I. Olivares, C. C. Morgan, Phylogeny and evolutionary patterns of South American Octodontoid rodents. *Acta Palaeontologica Polonica* **59**, 757–769 (2013).

35. D. H. Verzi, C. C. Morgan, A. I. Olivares, "The history of South American octodontoid rodents and its contribution to evolutionary generalisations" in *Evolution of the Rodents*, 1st Ed., P. G. Cox, L. Hautier, Eds. (Cambridge University Press, 2015), pp. 139–163.

36. D. H. Verzi, A. I. Olivares, C. C. Morgan, A. Álvarez, Contrasting phylogenetic and diversity patterns in octodontoid rodents and a new definition of the family Abrocomidae. *Journal of Mammalian Evolution* **23**, 93–115 (2016).

37. M. Arnal, M. E. Pérez, A new acaremyid rodent (Hystricognathi: Octodontoidea) from the middle Miocene of Patagonia (South America) and considerations on the early evolution of Octodontoidea. *Zootaxa* **3616**, 119–134 (2013).

38. M. Arnal, M. G. Vucetich, Main radiation events in Pan-Octodontoidea (Rodentia, Caviomorpha). *Zoological Journal of the Linnean Society* **175**, 587–606 (2015).

39. P.-H. Fabre, *et al.*, Mitogenomic phylogeny, diversification, and biogeography of South American spiny rats. *Molecular biology and evolution* **34**, 613–633 (2017).

40. C. J. Burgin, J. P. Colella, P. L. Kahn, N. S. Upham, How many species of mammals are there? *Journal of Mammalogy* **99**, 1–14 (2018).

41. Mammal Diversity Database, Mammal Diversity Database (2022) https:/doi.org/10.5281/zenodo.5945626 (July 11, 2022).

42. W. C. Tavares, L. M. Pessôa, H. N. Seuánez, Phylogenetic and size constrains on cranial ontogenetic allometry of spiny rats (Echimyidae, Rodentia). *Journal of Evolutionary Biology* **29**, 1752–1765 (2016).

43. W. C. Tavares, L. M. Pessôa, H. N. Seuánez, Changes in ontogenetic allometry and their role in the emergence of cranial morphology in fossorial spiny rats (Echimyidae, Hystricomorpha, Rodentia). *Journal of Mammalian Evolution*, 1–11 (2018).

44. P.-H. Fabre, *et al.*, Rodents of the Caribbean: origin and diversification of hutias unravelled by next-generation museomics. *Biology Letters* **10**, 20140266 (2014).

45. N. S. Upham, R. Borroto-Páez, Molecular phylogeography of endangered Cuban hutias within the Caribbean radiation of capromyid rodents. *Journal of Mammalogy* **98**, 950–963 (2017).

46. J. D. Carrillo, M. R. Sánchez-Villagra, Giant rodents from the Neotropics: diversity and dental variation of late Miocene neoepiblemid remains from Urumaco, Venezuela. *Palaontologische Zeitschrift* **89**, 1057–1071 (2015).

47. L. Kerber, F. R. Negri, J. Ferigolo, E. L. Mayer, A. M. Ribeiro, Modifications on fossils of neoepiblemids and other South American rodents. *Lethaia* **50**, 149–161 (2017).

48. L. Kerber, *et al.*, Postcranial morphology of the extinct rodent *Neoepiblema* (Rodentia: Chinchilloidea): insights into the paleobiology of neoepiblemids. *J Mammal Evol* **29**, 207–235 (2022).

49. L. L. Rasia, A. M. Candela, Upper molar morphology, homologies and evolutionary patterns of chinchilloid rodents (Mammalia, Caviomorpha). *Journal of Anatomy* **234**, 50–65 (2019).

50. L. Kerber, M. R. Sánchez-Villagra, Morphology of the middle ear ossicles in the rodent *Perimys* (Neoepiblemidae) and a comprehensive anatomical and morphometric study of the phylogenetic transformations of these structures in caviomorphs. *Journal of Mammalian Evolution* **26**, 407–422 (2019).

51. J. D. Ferreira, F. R. Negri, M. R. Sánchez-Villagra, L. Kerber, Small within the largest: brain size and anatomy of the extinct *Neoepiblema acreensis*, a giant rodent from the Neotropics. *Biology Letters* **16**, 20190914 (2020).

52. L. L. Rasia, A. M. Candela, C. Cañón, Comprehensive total evidence phylogeny of chinchillids (Rodentia, Caviomorpha): Cheek teeth anatomy and evolution. *Journal of Anatomy* **239**, 405–423 (2021).

53. M. R. Sánchez-Villagra, O. A. Aguilera, I. Horovitz, The anatomy of the world ’s largest extinct rodent. *Science* **301**, 1708–1710 (2003).

54. A. Rinderknecht, R. E. Blanco, The largest fossil rodent. *Proceedings of the Royal Society B: Biological Sciences* **275**, 923–928 (2008).

55. M. Geiger, L. A. B. Wilson, L. Costeur, R. Sánchez, M. R. Sánchez-Villagra, Diversity and body size in giant caviomorphs (Rodentia) from the northern Neotropics—a study of femoral variation. *Journal of Vertebrate Paleontology* **33**, 1449–1456 (2013).

56. R. K. Engelman, Resizing the largest known extinct rodents (Caviomorpha: Dinomyidae, Neoepiblemidae) using occipital condyle width. *R. Soc. open sci.* **9**, 220370 (2022).

57. A. R. Biknevicius, D. a. McFarlane, R. D. E. Macphee, Body size in *Amblyrhiza inundata* (Rodentia: Caviomorpha), an extinct megafaunal rodent from the Anguilla Bank, West Indies: estimates and implications. *American Museum Novitates* **3079**, 1–25 (1993).

58. R. D. E. MacPhee, Basicranial morphology and relationships of antillean Heptaxodontidae (Rodentia, Ctenohystrica, Caviomorpha). *Bulletin of the American Museum of Natural History* **363**, 1–70 (2011).

59. R. Woods, I. Barnes, S. Brace, S. T. Turvey, Ancient DNA suggests single colonization and within-archipelago diversification of caribbean caviomorph rodents. *Molecular Biology and Evolution* **38**, 84–95 (2021).

60. L. Da Cunha, *et al.*, The inner ear of caviomorph rodents: Phylogenetic implications and application to extinct West Indian taxa. *J Mammal Evol* (2023) https:/doi.org/10.1007/s10914-023-09675-3 (August 2, 2023).

61. D. Silvestro, *et al.*, Fossil data support a pre-Cretaceous origin of flowering plants. *Nature Ecology & Evolution 2021 5:4* **5**, 449–457 (2021).

62. T. Stadler, D. Kühnert, S. Bonhoeffer, A. J. Drummond, Birth–death skyline plot reveals temporal changes of epidemic spread in HIV and hepatitis C virus (HCV). *Proceedings of the National Academy of Sciences* **110**, 228–233 (2013).

63. F. J. Goin, M. A. Abello, L. Chornogubsky, "Middle Tertiary marsupials from central Patagonia (early Oligocene of Gran Barranca): understaing South America's *Grande Coupture*" in *The Paleontology of Gran Barranca. Evolution and Environmental Change through the Middle Cenozoic of Patagonia*, R. H. Madden, A. A. Carlini, M. G. Vucetich, R. F. Kay, Eds. (Cambridge University Press, 2010), pp. 69–105.

64. C. N. Garzione, *et al.*, Rise of the Andes. *Science* **320**, 1304–1307 (2008).

65. L. M. Boschman, Andean mountain building since the Late Cretaceous: A paleoelevation reconstruction. *Earth-Science Reviews* **220**, 103640 (2021).

66. N. S. Upham, R. Ojala-Barbour, J. Brito M, P. M. Velazco, B. D. Patterson, Transitions between Andean and Amazonian centers of endemism in the radiation of some arboreal rodents. *BMC evolutionary biology* **13**, 191 (2013).

67. C. L. Miranda, *et al.*, Diversification of Amazonian spiny tree rats in genus *Makalata* (Rodentia, Echimyidae): Cryptic diversity, geographic structure and drivers of speciation. *PLoS ONE* **17**, e0276475 (2022).

68. J. D. Carrillo, *et al.*, Disproportionate extinction of South American mammals drove the asymmetry of the Great American Biotic Interchange. *Proceedings of the National Academy of Sciences* **117**, 26281–26287 (2020).

69. L. Kerber, *et al.*, Tropical fossil caviomorph rodents from the southwestern Brazilian Amazonia in the context of the South American faunas: systematics, biochronology, and paleobiogeography. *Journal of Mammalian Evolution* **24**, 57–70 (2017).

70. I. Horovitz, M. R. Sánchez-Villagra, M. G. Vucetich, O. A. Aguilera, “Fossil rodents from the late Miocene Urumaco and middle Miocene Cumaca Formations, Venezuela” in *Urumaco & Venezuelan Paleontology. The Fossil Record of the Northern Neotropics*, M. R. Sánchez-Villagra, O. A. Aguilera, A. A. Carlini, Eds. (Indiana University Press, 2010), pp. 214–232.

71. C. Hoorn, *et al.*, Amazonia through time: Andean uplift, climate change, landscape evolution, and biodiversity. *Science* **330**, 927–931 (2010).

72. C. Hoorn, L. G. Lohmann, L. M. Boschman, F. L. Condamine, Neogene History of the Amazonian Flora: A perspective based on geological, palynological, and molecular phylogenetic data. *Annual Review of Earth and Planetary Sciences* **51**, 419–446 (2023).

73. C. Jaramillo, *et al.*, Miocene flooding events of western Amazonia. *Science Advances* **3** (2017).

74. R. Salas-Gismondi, *et al.*, A Miocene hyperdiverse crocodylian community reveals peculiar trophic dynamics in proto-Amazonian mega-wetlands. *Proceedings of the Royal Society B: Biological Sciences* **282**, 4–8 (2015).

75. T. M. Scheyer, *et al.*, Crocodylian diversity peak and extinction in the late Cenozoic of the northern Neotropics. *Nature communications* **4**, 1907 (2013).

76. S. T. Turvey, F. V. Grady, P. Rye, A new genus and species of ‘giant hutia’ (*Tainotherium valei*) from the Quaternary of Puerto Rico: an extinct arboreal quadruped? *Journal of Zoology* **270**, 585–594 (2006).

77. P. Raia, F. Carotenuto, F. Passaro, D. Fulgione, M. Fortelius, Ecological specialization in fossil mammals explains Cope’s rule. *The American Naturalist* **179**, 328–337 (2012).

78. M. Clauss, *et al.*, Herbivory and body size: allometries of diet quality and gastrointestinal physiology, and implications for herbivore ecology and dinosaur gigantism. *PLoS ONE* **8**, e68714 (2013).

79. A. H. Castillo, M. N. Cortinas, E. P. Lessa, Rapid diversification of South American tuco-tucos (*Ctenomys*; Rodentia, Ctenomyidae): contrasting mitochondrial and nuclear intron sequences. *Journal of Mammalogy* **86**, 170–179 (2005).

80. S. L. Gardner, New species of *Ctenomys* Blainville 1826: (Rodentia : Ctenomyidae) from the lowlands and central valleys of Bolivia. *Special Publications Museum of Texas Tech University* **62** (2014).

81. T. A. Spradling, S. V. Brant, M. S. Hafner, C. J. Dickerson, DNA data support a rapid radiation of pocket gopher genera (Rodentia: Geomyidae). *Journal of Mammalian Evolution* **11**, 105–125 (2004).

82. L. Van Valen, Body size and numbers of plants and animals. *Evolution* **27**, 27–35 (1973).

83. T. Gardezi, J. da Silva, Diversity in relation to body size in mammals: a comparative study. *The American Naturalist* **153**, 110–123 (1999).

84. J. Damuth, Population density and body size in mammals. *Nature* **290**, 699–700 (1981).

85. W. A. Calder, *Size, Function, and Life History* (Harvard University Press, 1984).

86. S. K. Lyons, F. A. Smith, S. K. M. Ernest, Macroecological patterns of mammals across taxonomic, spatial, and temporal scales. *Journal of Mammalogy* **100**, 1087–1104 (2019).

87. D. J. Bennett, H. Hettling, D. Silvestro, R. Vos, A. Antonelli, restez: create and query a local copy of GenBank in R. *Journal of Open Source Software* **3**, 1102 (2018).

88. D. J. Bennett, *et al.*, phylotaR: an automated pipeline for retrieving orthologous DNA sequences from GenBank in R. *Life* **8**, 20 (2018).

89. C. Camacho, *et al.*, BLAST+: architecture and applications. *BMC Bioinformatics* **10**, 421 (2009).

90. M. J. Sanderson, D. Boss, D. Chen, K. A. Cranston, A. Wehe, The PhyLoTA browser: processing GenBank for molecular phylogenetics research. *Systematic Biology* **57**, 335–346 (2008).

91. K. Katoh, K. Misawa, K. Kuma, T. Miyata, MAFFT: a novel method for rapid multiple sequence alignment based on fast Fourier transform. *Nucleic Acids Research* **30**, 3059–3066 (2002).

92. J. L. Steenwyk, T. J. B. Iii, Y. Li, X.-X. Shen, A. Rokas, ClipKIT: A multiple sequence alignment trimming software for accurate phylogenomic inference. *PLOS Biology* **18**, e3001007 (2020).

93. R. Lanfear, P. B. Frandsen, A. M. Wright, T. Senfeld, B. Calcott, PartitionFinder 2: new methods for selecting partitioned models of evolution for molecular and morphological phylogenetic analyses. *Molecular Biology and Evolution* **34**, 772–773 (2017).

94. A. Stamatakis, RAxML-VI-HPC: maximum likelihood-based phylogenetic analyses with thousands of taxa and mixed models. *Bioinformatics* **22**, 2688–2690 (2006).

95. R. Lanfear, B. Calcott, S. Y. W. Ho, S. Guindon, Partitionfinder: combined selection of partitioning schemes and substitution models for phylogenetic analyses. *Molecular biology and evolution* **29**, 1695–701 (2012).

96. R. Bouckaert, *et al.*, BEAST 2.5: An advanced software platform for Bayesian evolutionary analysis. *PLOS Computational Biology* **15**, e1006650 (2019).

97. T. Stadler, Sampling-through-time in birth–death trees. *Journal of Theoretical Biology* **267**, 396–404 (2010).

98. P. O. Lewis, A likelihood approach to estimating phylogeny from discrete morphological character data. *Systematic biology* **50**, 913–25 (2001).

99. N. F. Müller, R. Bouckaert, Coupled MCMC in BEAST 2 (2019) https:/doi.org/10.1101/603514 (April 7, 2022).

100. A. Rambaut, A. J. Drummond, D. Xie, G. Baele, M. A. Suchard, Posterior summarization in Bayesian phylogenetics using Tracer 1.7. *Systematic Biology* **67**, 901–904 (2018).

101. L. A. B. Wilson, Allometric disparity in rodent evolution. *Ecology and Evolution* **3**, 971–984 (2013).

102. U. Anders, W. von Koenigswald, I. Ruf, B. H. Smith, Generalized individual dental age stages for fossil and extant placental mammals. *Palaontologische Zeitschrift* **85**, 321–339 (2011).

103. S. Faurby, *et al.*, PHYLACINE 1.2: The phylogenetic atlas of mammal macroecology. *Ecology* **99**, 2626–2626 (2018).

104. S. Faurby, *et al.*, MegaPast2Future/PHYLACINE_1.2: PHYLACINE Version 1.2.1 (2020) https:/doi.org/10.5281/zenodo.3690867 (October 7, 2022).

105. J. L. Patton, U. F. J. Pardiñas, G. D 'Elía, Eds., *Mammals of South America, Volume 2. Rodents* (The University of Chicago Press, 2015).

106. Louise. Emmons, P.-Henri. Fabre, A review of the *Pattonomys/Toromys* clade (Rodentia, Echimyidae), with descriptions of a new *Toromys* species and a new genus. *American Museum Novitates* **3894** (2018).

107. V. Millien, H. Bovy, When teeth and bones disagree: body mass estimation of a giant extinct rodent. *Journal of Mammalogy* **91**, 11–18 (2010).

108. D. Silvestro, *et al.*, Early arrival and climatically-linked geographic expansion of New World monkeys from tiny African ancestors. *Systematic Biology* (2018) https:/doi.org/10.1093/sysbio/syy046.

109. Q. Zhang, R. H. Ree, N. Salamin, Y. Xing, D. Silvestro, Fossil-Informed Models Reveal a Boreotropical Origin and Divergent Evolutionary Trajectories in the Walnut Family (Juglandaceae). *Systematic Biology* **71**, 242–258 (2022).

110. E. Paradis, J. Claude, K. Strimmer, APE: Analyses of Phylogenetics and Evolution in R language. *Bioinformatics* **20**, 289–290 (2004).

111. A. Gavryushkina, D. Welch, T. Stadler, A. J. Drummond, Bayesian inference of sampled ancestor trees for epidemiology and fossil calibration. *PLOS Computational Biology* **10**, e1003919 (2014).

112. B. Allen, M. V. Volkova, T. Stadler, T. G. Vaughan, R. C. Warnock, Mechanistic phylodynamic models do not provide conclusive evidence that non-avian dinosaurs were in decline before their final extinction. *Cambridge Prisms: Extinction* (In press).

113. L. J. Revell, phytools: an R package for phylogenetic comparative biology (and other things). *Methods in Ecology and Evolution* **3**, 217–223 (2012).

114. S. Lê, J. Josse, F. Husson, FactoMineR: An R package for multivariate analysis. *J. Stat. Soft.* **25** (2008).

## Figures and Tables

**Figure 1.** Patterns of diversification and morphological evolution in Octodontoidea and Chinchilloidea. **A.** Phenogram of body mass evolution of extinct and extant lineages. The reconstruction of ancestral states was estimated with the fossilized Brownian motion model with trend using a sample of 100 phylogenetic trees, of which one is shown. The phenogram shows the range of body mass (log transformed) through time for each clade, the dots represent the extant species, and the colored bars show the range of body mass of extant species of both clades. The ancestral body mass was similar for both clades, but subsequently Chinchilloidea shows a higher body mass range through time, reaching the higher values in the Pliocene and Pleistocene and a decrease towards the present. **B.** Body mass disparity through time for Chinchilloidea and Octodontoidea. Disparity was estimated as the variance of body mass of each clade in time bins of 1 Ma. Notice that Chinchilloidea had a higher body mass variance during most of the Paleogene and Neogene and only after the Pliocene the variance of body mass of Chinchilloidea is smaller than in Octodontoidea. **C.** Violin plots of the of rates of body mass evolution, with significant higher rates for Chinchilloidea. **D.** Violin plots of the trend parameter estimated for both clades. The model provides some support for a trend in body mass evolution in Chinchilloidea (trend parameter values > 0), but not in Octodontoidea.

**Figure 2.** Diversification dynamics of Chinchilloidea (blue) and Octodontoidea (red) through time. **A.** Lineage through time (LTT) plot. The solid lines and the shaded areas represent the mean and the 95% credible interval, respectively, of the number of species (log transformed) trough time for the sample of 100 phylogenetic trees. The two clades had similar diversity trajectories until the beginning of the Miocene, when Octodontoidea shows a trend of increasing diversity until the present, whereas Chinchilloidea diversity stagnate and decrease after the Pleistocene. **B.** Diversification through time. Skyline plot showing the diversification rates for each clade estimated for the sample of 100 trees for the following time bins: Paleogene; Oligocene; early, middle and late Miocene, Pliocene and Quaternary (Pleistocene and Holocene). Notice the higher diversification rates of Octodontoidea in the late Miocene and Quaternary. Abbreviations: Eo=Eocene; Ol=Oligocene, Mio=Miocene, Pli=Pliocene, Ple=Pleistocene.

**Figure 3.** Morphospace occupation of extant Chinchilloidea (blue) and Octodontoidea (red). **A.** Cranial measurements taken on specimens representing extant species, used to estimated cranial morphospace. Cranium of the plains viscacha (*Lagostomus maximus*; NMNH 172852) in ventral (top), dorsal (middle) and lateral (bottom) views. Measurement numbers correspond to Table S1. **B.** Frequency histogram of the morphospace occupation (measured as the area of the convex hull) for 100 subsamples of five species of Octodontoidea (equal to the number of Chinchilloidea) choose at random. The red line shows the morphospace area of Chinchilloidea (x = 3.1), and the gray line shows the median of the 100 Octodontoidea subsamples (x = 4.3). **C.** Cranial phylomorphospace showing the first two principal components (PC) of the PCA performed on the cranial and body mass traits of 33 Octodontoidea and five Chinchilloidea extant species. Notice that Chinchilloidea occupies a considerable portion of the morphospace in comparison with Octodontoidea, despite having a much lower number of species.

**Table 1.** Body mass evolution in Octodontoidea and Chinchilloidea. Rates of body mass (BM) evolution estimated with the fossilized Brownian motion model with and without trend, where the latter evaluates the presence of positive or negative trends. The mean likelihood of each model and the posterior probability of the trend parameter is also presented. CI = credible interval.

| **No trend** | **BM rates** | | | | |
|---|---|---|---|---|---|
| | Mean | 95% HDI | | | |
| Octodontoidea | 0.0164 | 0.0089 - 0.0287 | | | |
| Chinchilloidea | 0.0743 | 0.0265 - 0.1349 | | | |
| **Trend** | **BM rates** | | **Trend parameter** | | |
| | Mean | 95% HDI | Mean | 95% HDI | Posterior probability |
| Octodontoidea | 0.0163 | 0.0087 - 0.0283 | -0.0063 | (-0.0235) - 0.0107 | 0.2233 |
| Chinchilloidea | 0.0719 | 0.0259 - 0.1280 | 0.0351 | (-0.0093) - 0.0794 | 0.9391 |
| Ratio (Chinchilloidea / Octodontoidea) | 4.8169 | 0.9337 - 9.1446 | | | |

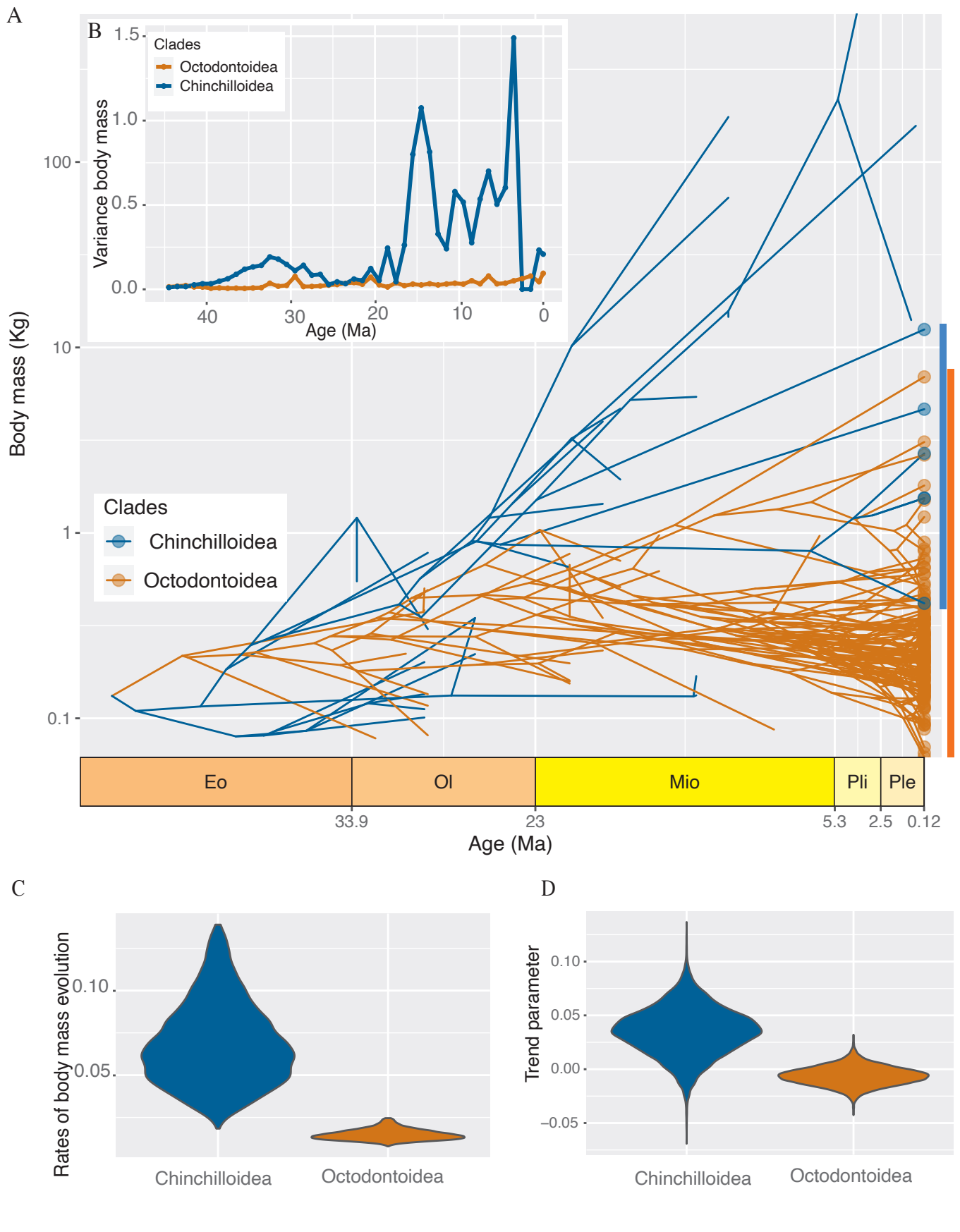
A
B
Clades
Octodontoidea
Chinchilloidea
Variance body mass
1.5
1.0
0.5
0.0
40
30
20
10
0
Age (Ma)
Body mass (Kg)
100
10
1
0.1
Clades
Chinchilloidea
Octodontoidea
Eo
Ol
Mio
Pli
Ple
33.9
23
5.3
2.5
0.12
Age (Ma)
C
Rates of body mass evolution
0.10
0.05
Chinchilloidea
Octodontoidea
D
Trend parameter
0.10
0.05
0.00
−0.05
Chinchilloidea
Octodontoidea

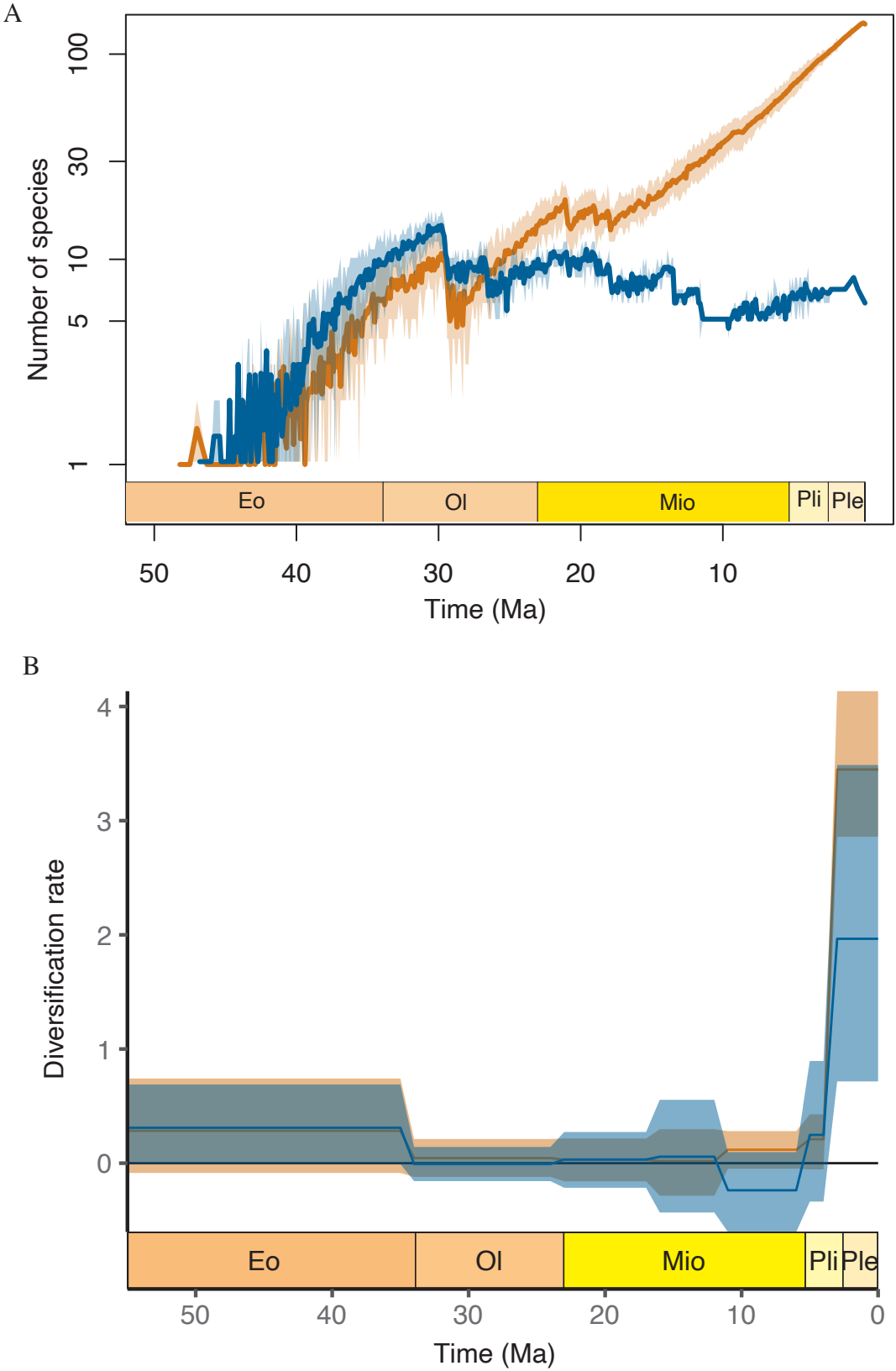
A
Number of species
100
30
10
5
1
Eo
Ol
Mio
Pli
Ple
50
40
30
20
10
Time (Ma)
B
Diversification rate
4
3
2
1
0
Eo
Ol
Mio
Pli
Ple
50
40
30
20
10
0
Time (Ma)

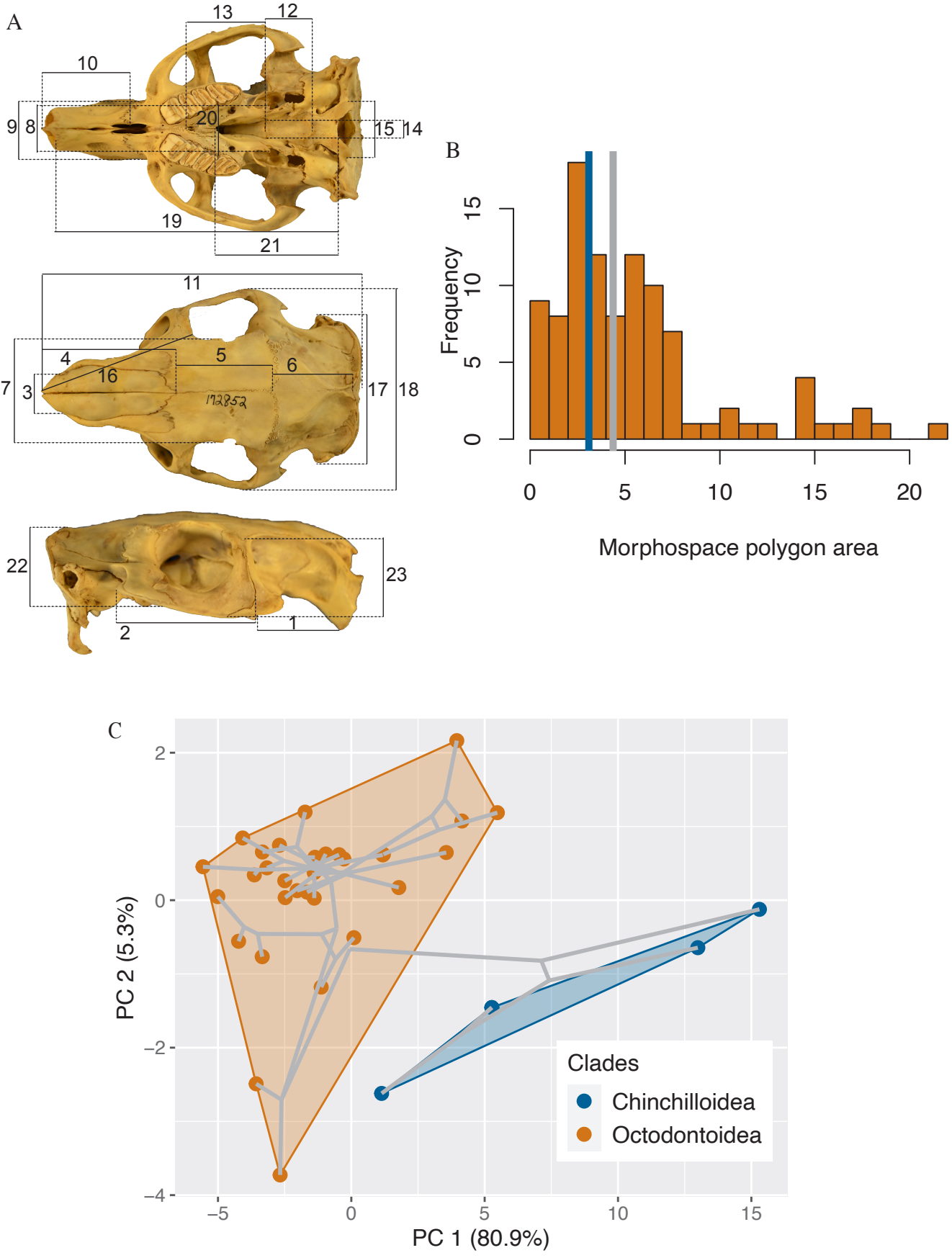
A
13
12
10
9
8
20
15
14
19
21
11
4
16
5
6
7
3
17
18
22
23
2
1
B
Frequency
0
5
10
15
0
5
10
15
20
Morphospace polygon area
C
2
0
−2
−4
−5
0
5
10
15
PC 2 (5.3%)
PC 1 (80.9%)
Clades
Chinchilloidea
Octodontoidea

# Supporting Information for
# Decoupled diversity and disparity after faunistic turnover in caviomorph rodents

Juan D. Carrillo*[1,2], María F. Torres Jiménez[3], Francisco J. Urrea-Barreto[4,5], Alexandre Antonelli[2,6,7,8], Christine Bacon[2], Søren Faurby[2], Daniele Silvestro[1,2]

1. Department of Biology, University of Fribourg, and Swiss Institute of Bioinformatics, Fribourg, CH1700, Switzerland.
2. Department of Biological and Environmental Sciences, and Gothenburg Global Biodiversity Centre, University of Gothenburg, Box 461, SE 405 30 Gothenburg, Sweden.
3. Institute of Biosciences, Life Sciences Center, Vilnius University, Vilnius, Lithuania.
4. Consejo Nacional de Investigaciones Científicas y Técnicas (CONICET), Museo Paleontológico Egidio Feruglio, Trelew, U9100GYO, Argentina.
5. Smithsonian Tropical Research Institute, 0843-03092 Balboa, Panama.
6. Royal Botanic Gardens, Kew, Richmond, Surrey, TW9 3AE, UK.
7. Wuhan Botanic Garden, Chinese Academy of Sciences, Wuhan, China.
8. Department of Biology, University of Oxford South Parks Road, Oxford, OX1 3RB, UK.

Juan D. Carrillo
Email: juan.carrillo@unifr.ch

The Datasets and code can be consulted and downloaded in the following SwitchDrive link:
https://drive.switch.ch/index.php/s/fULTN4t4Sqf2f1t

## Supporting Materials and Methods

**Phylogenetic relationships of extant species.** To test the congruence of the phylogenetic relationships inferred from the molecular alignment we obtained with previous phylogenies of Caviomorpha, ae used raxmlGUI 2.0 (1) to infer a maximum likelihood phylogenetic analyses of the extant species of Octodontoidea and Chinchilloidea. The resulting phylogeny (Fig. S1) was consistent with previous studies on the phylogenetic relationships of caviomorphs (2). An analysis using one partition (Fig. S2) yielded a topology congruent with the one obtained using the 16 partitions identified with PartitionFinder2 (Fig. S1). To improve the analytical tractability of our subsequent analyses, we used a single partition for the molecular matrix in the time-calibrated phylogenetic inference.

**Taxonomic constraints for time-calibrated phylogeny.** Due to the relative high number of fossil species included in the Bayesian time-calibrated analyses, we set several taxonomic constraints in order for the independent runs to converge. We constrained all the fossil species of the same genus as monophyletic. In addition, we set monophyletic constraints for the following clades: Abrocomidae (2), Acaremyidae (3–5), Adelphomyidae (5), Capromyidae (2), Capromyidae + Echimyidae (2), Dinomyidae (5, 6), Neoepiblemidae (7), Chinchillidae + Neoepiblemidae (5, 7), Octodontidae (2, 5, 8), Octodontoidea and Chinchilloidea (Table S4).

**Imputation of cranial trait missing data.** Two species for which only one specimen was available in museum collections to measure had missing data: *Geocapromys ingrahami* (missing data for six measurements), and *Santamartamys rufodorsalis* (missing data for one measurement). We used the TDIP package (9) to impute the missing data with phylogenetic imputation methods. We used four different approaches: phylogenetic imputation based on a Markov model of trait evolution (phylopars), non-parametric random forest (missForest), k-nearest neighbour (kNN), and multinomial logistic regression (MICE) (9). The four methods generated similar values for the missing data and for subsequent analyses we used the average of the four methods.

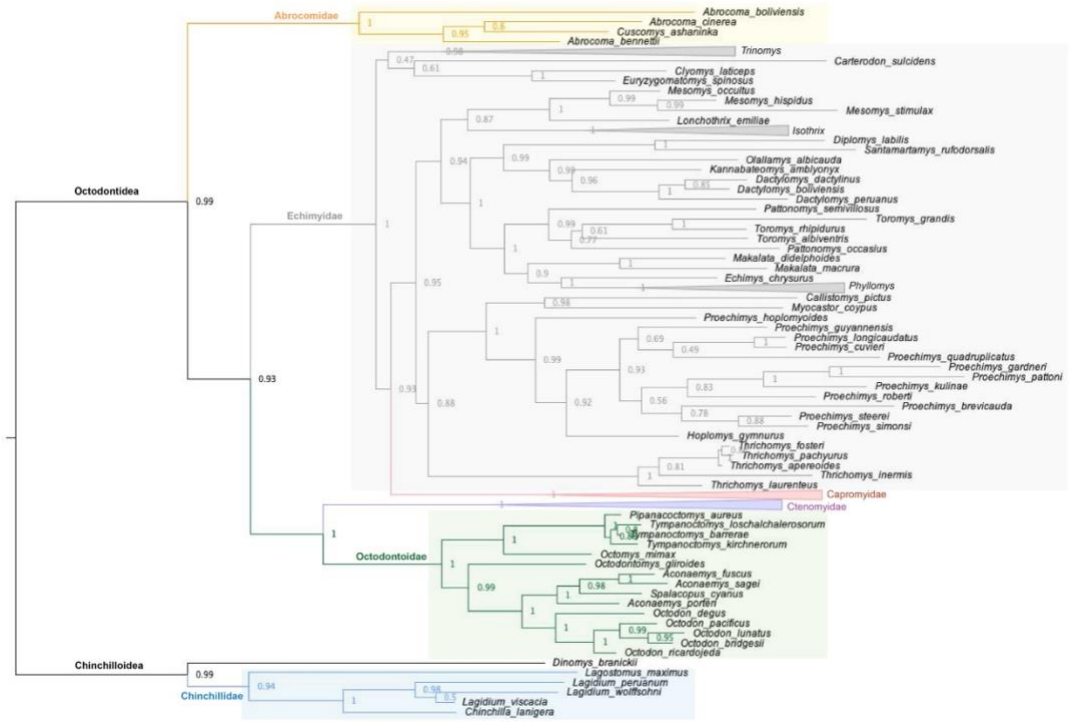


**Fig. S1.** Phylogenetic relationships of extant Chinchilloidea and Octodontoidea. Consensus tree obtained from the maximum likelihood analysis of the molecular supermatrix using 16 partitions, as identified by PartitionFinder2. Node values denote bootstrap support.

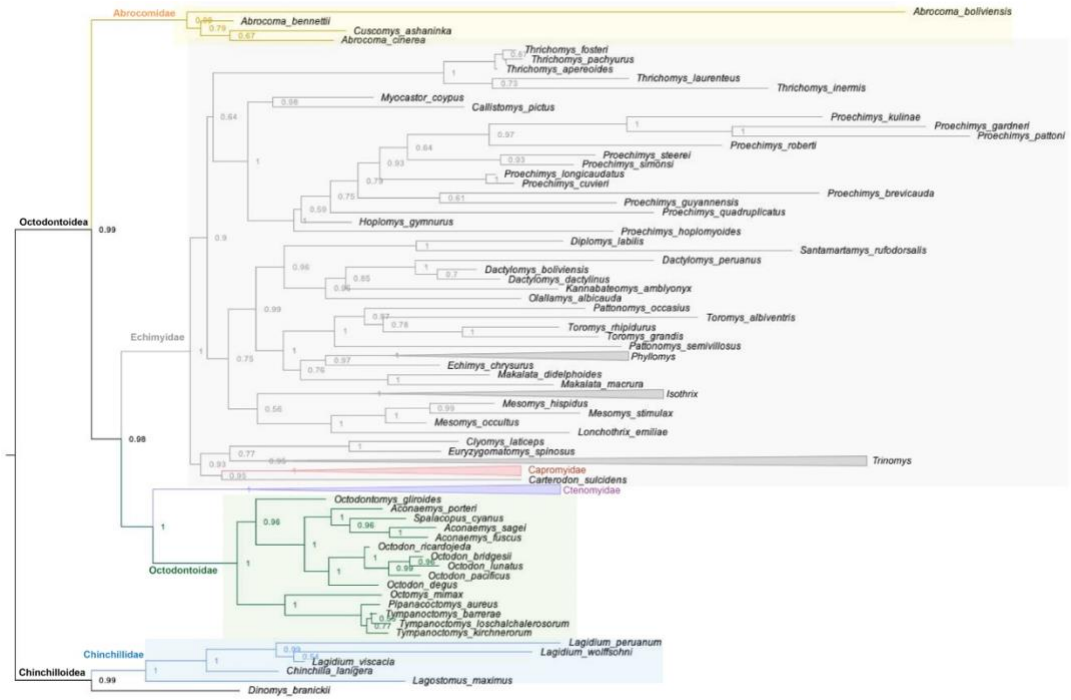


**Fig. S2.** Phylogenetic relationships of extant Chinchilloidea and Octodontoidea. Consensus tree obtained from the maximum likelihood analysis of the molecular supermatrix using one partition. Node values denote bootstrap support.

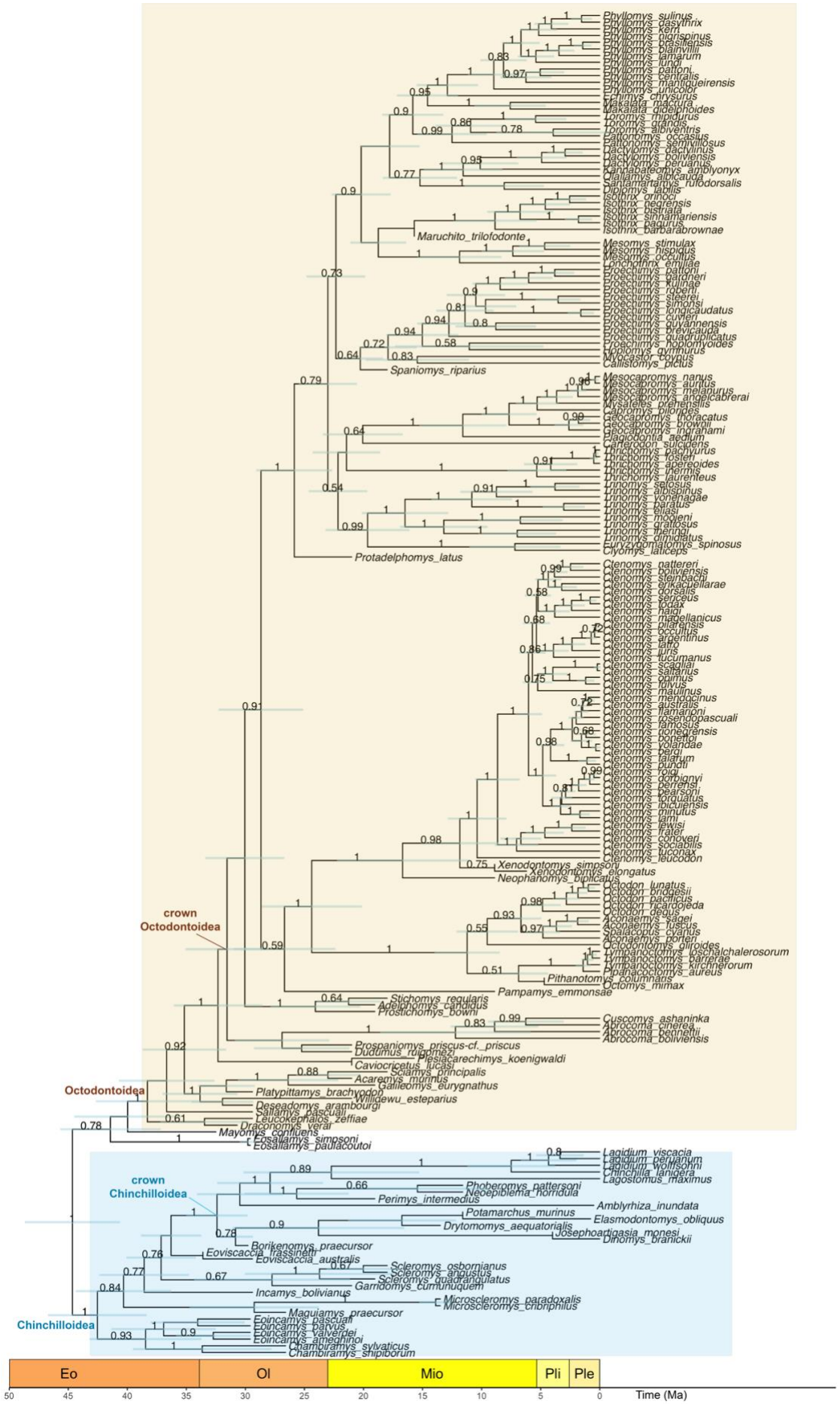
Phyllomys_sulinus
Phyllomys_dasythrix
Phyllomys_kerri
Phyllomys_nigrispinus
Phyllomys_brasiliensis
Phyllomys_blainvillii
Phyllomys_lamarum
Phyllomys_lundi
Phyllomys_pattoni
Phyllomys_centralis
Phyllomys_mantiqueirensis
Phyllomys_unicolor
Echimys_chrysurus
Makalata_macrura
Makalata_didelphoides
Loromys_rhipidurus
Loromys_grandis
Loromys_albiventris
Pattonomys_occasius
Pattonomys_semivillosus
Dactylomys_dactylinus
Dactylomys_boliviensis
Dactylomys_peruanus
Kannabateomys_amblyonyx
Olallamys_albicauda
Santamartamys_rufodorsalis
Diplomys_labilis
Isothrix_orinoci
Isothrix_negrensis
Isothrix_bistriata
Isothrix_sinnamariensis
Isothrix_pagurus
Isothrix_barbarabrownae
Maruchito_trilofodonte
Mesomys_stimulax
Mesomys_hispidus
Mesomys_occultus
Lonchothrix_emiliae
Proechimys_patorni
Proechimys_gardneri
Proechimys_kulinae
Proechimys_roberti
Proechimys_steerei
Proechimys_simonsi
Proechimys_longicaudatus
Proechimys_cuvieri
Proechimys_guyannensis
Proechimys_brevicauda
Proechimys_quadruplicatus
Proechimys_hoplomyoides
Hoplomys_gymnurus
Mycaster_coypus
Callistomys_pictus
Spaniomys_riparius
Mesocapromys_nanus
Mesocapromys_auritus
Mesocapromys_melanurus
Mesocapromys_angelcabrerai
Mysateles_prehensilis
Capromys_pilorides
Geocapromys_thoracatus
Geocapromys_browni
Geocapromys_ingrahami
Plagiodontia_aedium
Carteodon_sitiadens
Trichomys_pachyurus
Trichomys_fosteri
Trichomys_apereoides
Trichomys_inermis
Trichomys_laurentius
Trinomys_setosus
Trinomys_albispinus
Trinomys_yonenagae
Trinomys_paratus
Trinomys_eliasi
Trinomys_moojeni
Trinomys_gratiosus
Trinomys_therezae
Trinomys_dimidiatus
Euryzygomatomys_spinosus
Cryomys_laticeps
Protadelphomys_latus
Ctenomys_nattereri
Ctenomys_boliviensis
Ctenomys_steinbachi
Ctenomys_brikacellarae
Ctenomys_dorsalis
Ctenomys_sericeus
Ctenomys_lodax
Ctenomys_haigi
Ctenomys_magellanicus
Ctenomys_pilarensis
Ctenomys_occultus
Ctenomys_argentinus
Ctenomys_latro
Ctenomys_juris
Ctenomys_tucumanus
Ctenomys_scagliai
Ctenomys_saltarius
Ctenomys_opimus
Ctenomys_fulvus
Ctenomys_maulinus
Ctenomys_mendocinus
Ctenomys_australis
Ctenomys_flamarioni
Ctenomys_rosendopascuali
Ctenomys_famosus
Ctenomys_conegrensis
Ctenomys_bonettoi
Ctenomys_yolandae
Ctenomys_sergi
Ctenomys_talarum
Ctenomys_pundti
Ctenomys_roigi
Ctenomys_dorbignyi
Ctenomys_perrensi
Ctenomys_bearsoni
Ctenomys_torquatus
Ctenomys_lilloiensis
Ctenomys_minutus
Ctenomys_lami
Ctenomys_flexuosi
Ctenomys_frater
Ctenomys_conoveri
Ctenomys_sociabilis
Ctenomys_tuconax
Ctenomys_leucodon
Xenodontomys_simpsoni
Xenodontomys_elongatus
Neophanomys_biplicatus
Octodon_lunatus
Octodon_bridgesii
Octodon_pacificus
Octodon_ricardoeida
Octodon_degus
Aconaemys_sagei
Aconaemys_fuscus
Spalacopus_cyanus
Aconaemys_porteri
Octodontomys_gliroides
Tympanoctomys_loschalcherosorum
Tympanoctomys_barrerae
Tympanoctomys_kirchnerorum
Pipanacoctomys_aureus
Pithanotomys_columnaris
Octomys_mimax
Pampamys_emmonsae
Stichomys_regularis
Adelphomys_candidus
Prostichomys_bowni
Cuscomys_ashaninka
Abrocoma_cinerea
Abrocoma_bennettii
Abrocoma_boliviensis
Prospaniomys_priscus-cf._priscus
Dudumus_ruigomezi
Plesiacarechimys_koenigwaldi
Caviocricetus_lucasi
Sciamys_principalis
Acaremys_murinus
Galileomys_eurygnathus
Platypittamys_brachyodon
Willidewu_esteparius
Deseadomys_arambourgi
Saltamys_descussi
Leucochaetus_zeffiae
Draconomys_verai
Mayomys_confluens
Eosallamys_simpsoni
Eosallamys_paulacoutoi
Lagidium_viscacia
Lagidium_peruanum
Lagidium_wolffsohni
Chinchilla_lanigera
Lagostomus_maximus
Phoberomys_pattersoni
Neoepiblema_horridula
Perimys_intermedius
Amblyrhiza_inundata
Potamarchus_murinus
Elasmodontomys_obliquus
Drytomomys_aequatorialis
Josephoaenasia_monesi
Dinomys_branickii
Borikenomys_praecursor
Eoviscaccia_frassinetti
Eoviscaccia_australis
Scleromys_osbornianus
Scleromys_angustus
Scleromys_quadrangulatus
Garridomys_cumunuquem
Incamys_bolivianus
Microscleromys_paradoxalis
Microscleromys_cribriphilus
Maquiamys_praecursor
Eoincamys_pascuali
Eoincamys_parvus
Eoincamys_valverdei
Eoincamys_ameghinoi
Chambiramys_sylvaticus
Chambiramys_shipiborum
crown Octodontoidea
Octodontoidea
crown Chinchilloidea
Chinchilloidea
Eo
Ol
Mio
Pli
Ple
50
45
40
35
30
25
20
15
10
5
0
Time (Ma)

**Fig. S3.** Phylogenetic relationships of extinct and extant Chinchilloidea (shown in light orange) and Octodontoidea (shown in light green). Maximum clade credibility tree. The numbers show the clade posterior values larger than 0.5. The red horizontal bars are the 95% highest probability density intervals for the divergence times. Abbreviations: Eo = Eocene; Ol = Oligocene; Mio = Miocene; Pli = Pliocene; Ple = Pleistocene; (Holocene not shown). Ma = millions of years.

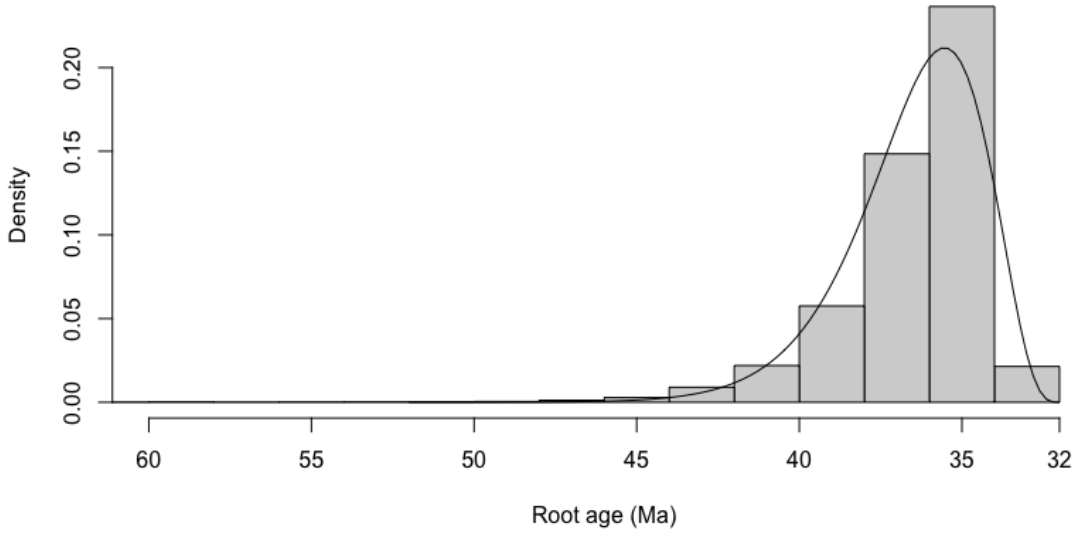


**Fig. S4.** Density plot of the estimation of the root age for Chinchilloidea + Octodontoidea using the Bayesian Brownian bridge model showing the gamma distribution used set the prior of the age of origin in the time-calibrated phylogenetic analysis.

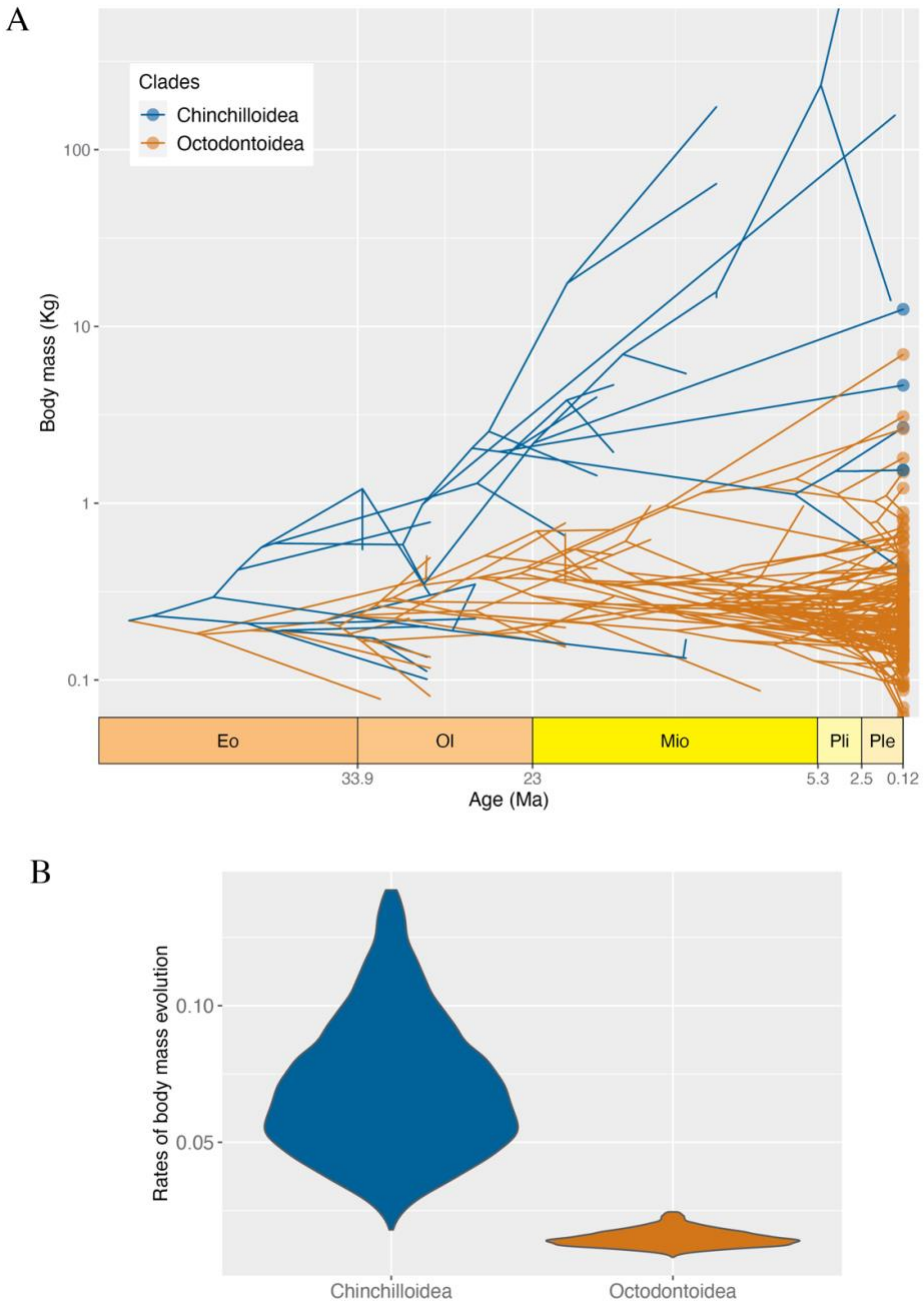


**Fig. S5.** Body mass evolution of extinct and extant lineages of Octodontoidea and Chinchilloidea, and reconstruction of ancestral states estimated with the fossilized Brownian motion model without trend. **A.** The shade areas show the range of body mass (log transformed) through time for each clade and the root (light gray), the dots represent the body mass of the tips (extinct and extant species) and nodes across a sample of 100 phylogenetic trees. **B.** Violin plots of the of rates of body mass evolution, with significant higher rates for Chinchilloidea. Abbreviations: Eo = Eocene; Ol = Oligocene; Mio = Miocene; Pli = Pliocene; Ple = Pleistocene. Ma = millions of years.

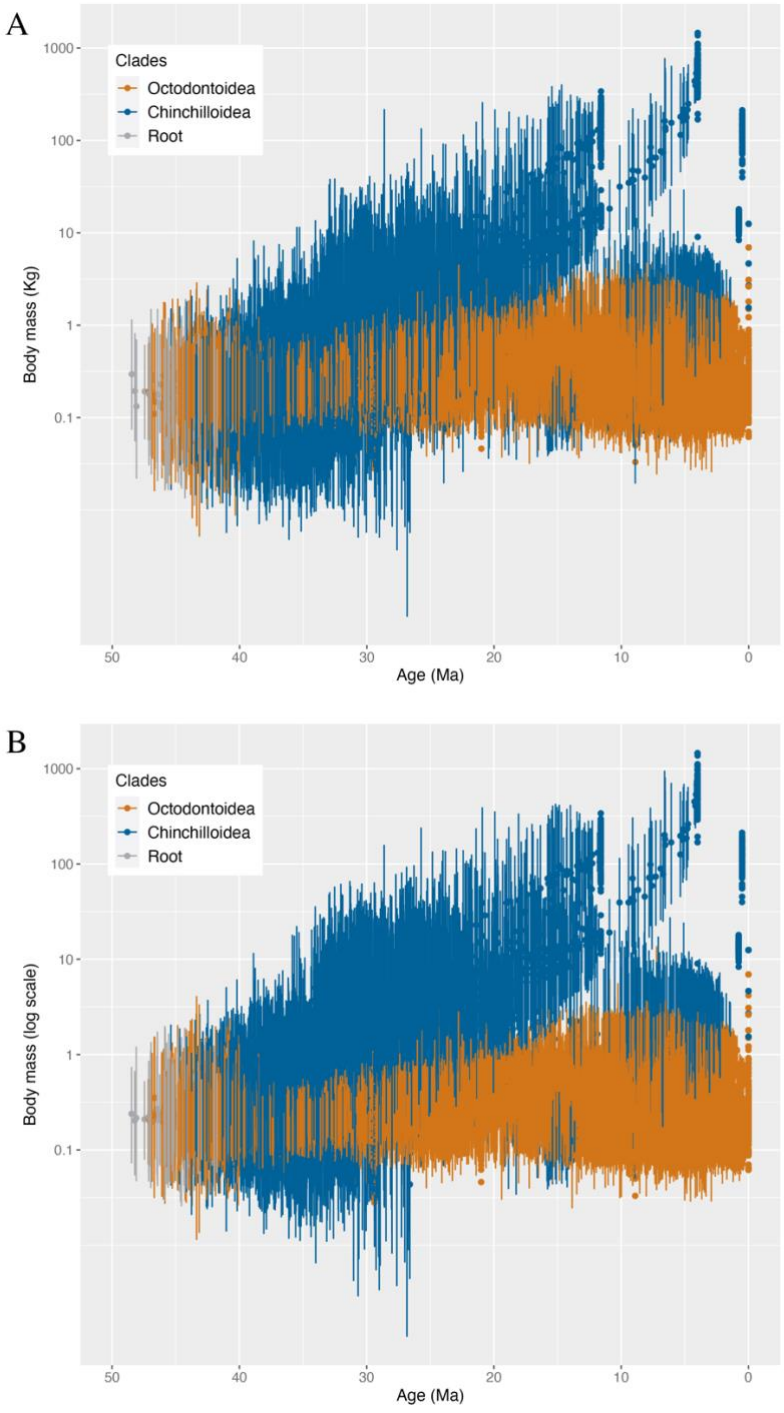


**Fig. S6.** Body mass evolution of extinct and extant lineages of Octodontoidea and Chinchilloidea, and reconstruction of ancestral states. A (top). Body mass estimated with the fossilized Brownian motion model without trend. B (bottom). Body mass estimated with the fossilized Brownian motion model with trend The shade areas show the range of body mass (log transformed) through time for each clade and the root (light gray), the dots represent the body mass of the tips (extinct and extant species) and nodes across a sample of 100 phylogenetic trees, and the bars represent the 95% credible interval of the body size estimation for each dot.

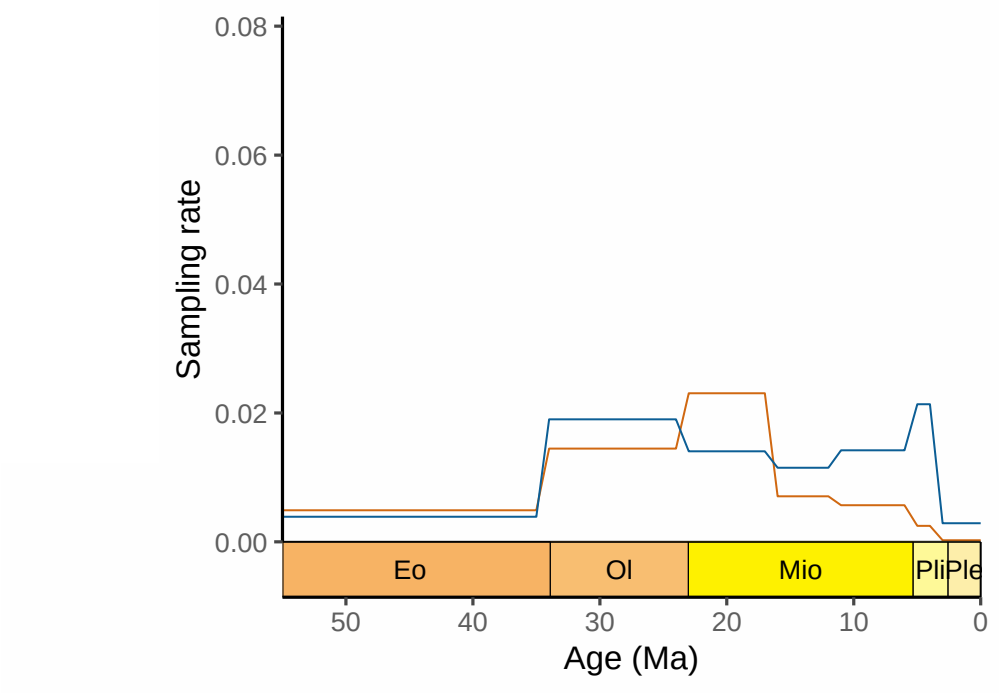


**Fig. S7.** Fossil sampling estimated for Chinchilloidea and Octodontoidea. Fossil sampling rates estimated with the Fossilized Birth-Death Skyline model for the sample of 100 phylogenetic trees for the following time bins: Eocene; Oligocene; early, middle and late Miocene, Pliocene and Quaternary. Notice the higher diversification rates of Octodontoidea in the late Miocene and Quaternary. Abbreviations: Eo = Eocene; Ol = Oligocene; Mio = Miocene; Pli = Pliocene; Ple = Pleistocene. Ma = millions of years.

**Table S1.** Cranial measurements taken on specimens representing extant species of Octodontoidea and Chinchilloidea. Measurements numbers and abbreviations correspond to (10) and (11, 12) respectively.

| Measurement | Wilson (2013) | Tavares et al (2016; 2018) |
|---|---|---|
| Length of diastema | 1 | LD |
| Jugal length | 2 | |
| Nasal width | 3 | |
| Nasal length | 4 | LN |
| Frontal length | 5 | LF |
| Parietal length | 6 | Lpar |
| Interorbital width | 7 | IOC |
| Palatal width | 8 | |
| Premaxilla width | 9 | WR |
| Premaxilla length | 10 | |
| Skull length | 11 | GSL |
| Basisphenoid length | 12 | |
| Palatal length | 13 | |
| Basisphenoid width | 15 | |
| Occipital condyles width | 17 | |
| Length of rostrum | | LR |
| Width of mastoids | | WM |
| Width of zygomatic arches | | WZ |
| Basilar length | | BL |
| Width of maxillaries on M3 | | Wmax |
| Post-palatal length | | PPL |
| Height of braincase | | HB |
| Height of zygomatic plate | | HZP |

**Table S2.** Taxonomic list of NCBI Taxids queried in GenBank.

| Clade | Family | Genus | NCBI Taxid |
|---|---|---|---|
| Chinchilloidea | Chinchillidae | *Chinchilla* | 10151 |
| | | *Lagidium* | 84622 |
| | | *Lagostomus* | 10153 |
| | Dinomyidae | *Dinomys* | 108857 |
| Octodontoidea | Abrocomidae | *Abrocoma* | 108854 |
| | | *Cuscomys* | 1567516 |
| | Octodontidae | *Aconaemys* | 183513 |
| | | *Octodon* | 10159 |
| | | *Octomys* | 135582 |
| | | *Pipanacoctomys* | 227729 |
| | | *Salinoctomys* | 1567519 |
| | | *Spalacopus* | 61879 |
| | | *Tympanoctomys* | 61881 |
| | | *Octodontomys* | 170739 |
| | Ctenomyidae | *Ctenomys* | 33551 |
| | Echimyidae | *Callistomys* | 1567506 |
| | | *Carterodon* | 1567512 |
| | | *Clyomys* | 176497 |
| | | *Dactylomys* | 30617 |
| | | *Diplomys* | 1567521 |
| | | *Echimys* | 30620 |
| | | *Euryzygomatomys* | 43324 |
| | | *Hoplomys* | 176500 |
| | | *Isothrix* | 30623 |
| | | *Kannabateomys* | 176502 |
| | | *Lonchothrix* | 176504 |
| | | *Makalata* | 490305 |
| | | *Mesomys* | 30626 |
| | | *Myocastor* | 10156 |
| | | *Olallamys* | 1400527 |
| | | *Pattonomys* | 1567523 |
| | | *Phyllomys* | 466156 |
| | | *Proechimys* | 10162 |
| | | *Santamartamys* | 1568969 |
| | | *Thrichomys* | 43326 |
| | | *Trinomys* | 42826 |
| | | *Toromys* | 1744847 |
| | Capromyidae | *Capromys* | 34841 |

| | | |
|---|---|---|
| | *Geocapromys* | 1543401 |
| | *Mesocapromys* | 1567508 |
| | *Mysateles* | 1543404 |
| | *Plagiodontia* | 1163664 |

**Table S3.** Partition scheme for phylogenetic analysis as obtained from PartitionFinder2 (13).

| Subset | Best Model | Partition names | Subset sites |
|---|---|---|---|
| 1 | GTR+I+G | mtDNA_0 | 1-11925 |
| 2 | GTR+I+G | nDNA_19 | 11926-12628 |
| 3 | GTR+G | nDNA_21 | 12629-13439 |
| 4 | GTR+I+G | nDNA_28, nDNA_96, nDNA_171, nDNA_217 | 13440-14276<br>19041-19877<br>27166-28031<br>32026-32372 |
| 5 | GTR+I+G | nDNA_39 | 14277-14536 |
| 6 | GTR+I+G | nDNA_219, nDNA_42 | 32933-33850<br>14537-15465 |
| 7 | GTR+I+G | nDNA_46 | 15466-16334 |
| 8 | GTR+I+G | nDNA_50 | 16335-17070 |
| 9 | GTR+I+G | nDNA_57, nDNA_97 | 17071-17952<br>19878-20573 |
| 10 | GTR+I+G | nDNA_159, nDNA_134, nDNA_216, nDNA_59 | 24849-25880<br>21577-22429<br>31177-32025<br>17953-19040 |
| 11 | GTR+I+G | nDNA_98 | 20574-21576 |
| 12 | GTR+I+G | nDNA_203, nDNA_138 | 30460-31176<br>22430-23403 |
| 13 | GTR+G | nDNA_178, nDNA_139, nDNA_170, nDNA_176 | 29145-29700<br>23404-24331<br>26633-27165<br>28032-28364 |
| 14 | GTR+G | nDNA_179, nDNA_140 | 29701-29961<br>24332-24848 |
| 15 | GTR+G | nDNA_190, nDNA_160, nDNA_177 | 29962-30190<br>25881-26632<br>28365-29144 |
| 16 | GTR+G | nDNA_202, nDNA_218 | 30191-30459<br>32373-32932 |

**Table S4.** Age ranges (in millions of years [Ma]) of the extinct species of Chinchilloidea and Octodontoidea included in the phylogenetic analysis. SALMA = South American Land Mammal Age.

| Species | Max Age | Min Age | Epoch/SALMA | Clade | References |
|---|---|---|---|---|---|
| *Eoincamys pascuali* | 29.6 | 25 | Early Oligocene | Chinchilloidea | (14–16) |
| *Eoincamys ameghinoi* | 29.6 | 25 | Early Oligocene | Chinchilloidea | (14–16) |
| *Eoincamys valverdei* | 29.6 | 25 | Early Oligocene | Chinchilloidea | (14–16) |
| *Eoincamys parvus* | 29.6 | 25 | Early Oligocene | Chinchilloidea | (14–16) |
| *Incamys bolivianus* | 29.4 | 24.2 | Deseadan | Chinchilloidea | (17–19) |
| *Scleromys quadrangulatus* | 19.04 | 17.5 | Pinturan | Chinchilloidea | (17, 20, 21) |
| *Scleromys osbornianus* | 18 | 15.6 | Santacrucian | Chinchilloidea | (20, 22) |
| *Scleromys angustus* | 18 | 15.6 | Santacrucian | Chinchilloidea | (20, 22) |
| *Maquiamys praecursor* | 26.6 | 23.03 | Late Oligocene | Chinchilloidea | (16, 23) |
| *Microscleromys paradoxalis* | 13.5 | 11.8 | Laventan | Chinchilloidea | (24, 25) |
| *Microscleromys cribriphilus* | 13.5 | 11.8 | Laventan | Chinchilloidea | (24, 25) |
| *Drytomomys aequatorialis* | 13.5 | 11.8 | Laventan | Chinchilloidea | (25, 26) |
| *Potamarchus murinus* | 11.6 | 5.3 | Late Miocene | Chinchilloidea | (27) |
| *Neoepiblema horridula* | 11.6 | 5.3 | Late Miocene | Chinchilloidea | (28) |
| *Garridomys curnunuquem* | 21 | 20.1 | Colhuehuapian | Chinchilloidea | (17, 29) |
| *Eoviscaccia frassinetti* | 33.6 | 31.6 | Tinguiririan | Chinchilloidea | (17, 30) |

| | | | | | |
|---|---|---|---|---|---|
| *Eoviscaccia australis* | 29.4 | 20.1 | Deseadan-Colhuehuapian | Chinchilloidea | (17, 30–32) |
| *Perimys intermedius* | 19.04 | 17.5 | Pinturan | Chinchilloidea | (17, 21, 33) |
| *Draconomys verai* | 30.7 | 29.5 | Pre-Deseadan | Octodontoidea | (17, 34) |
| *Platypittamys brachyodon* | 29.4 | 24.2 | Deseadan | Octodontoidea | (17, 35) |
| *Eosallamys paulacoutoi* | 29.6 | 25 | Early Oligocene | Caviomorpha | (14–16) |
| *Eosallamys simpsoni* | 29.6 | 25 | Early Oligocene | Caviomorpha | (14–16) |
| *Sallamys pascuali* | 29.4 | 24.2 | Deseadan | Octodontoidea | (17, 36) |
| *Prospaniomys priscus* | 21 | 20.1 | Colhuehuapian | Octodontoidea | (17, 32, 37) |
| *Spaniomys riparius* | 18 | 15.6 | Santacrucian | Octodontoidea | (22, 38) |
| *Protadelphomys latus* | 21 | 20.1 | Colhuehuapian | Octodontoidea | (17, 32) |
| *Willidewu esteparius* | 21 | 20.1 | Colhuehuapian | Octodontoidea | (17, 32) |
| *Xenodontomys simpsoni* | 8.9 | 5.1 | Late Miocene | Octodontoidea | (39, 40) |
| *Xenodontomys elongatus* | 6.2 | 5.1 | Late Miocene | Octodontoidea | (39, 40) |
| *Caviocricetus lucasi* | 21 | 20.1 | Colhuehuapian | Octodontoidea | (17, 32) |
| *Acaremys murinus* | 21 | 15.6 | Colhuehuapian-Santacrucian | Octodontoidea | (4) |
| *Plesiacarechimys koenigwaldi* | 15.7 | 14 | Colloncuran | Octodontoidea | (41, 42) |
| *Dudumus ruigomezi* | 21 | 20.1 | Colhuehuapian | Octodontoidea | (17, 43) |

| | | | | | |
|---|---|---|---|---|---|
| *Galileomys eurygnathus* | 19.04 | 17.5 | Pinturan | Octodontoidea | (17, 44, 45) |
| *Sciamys principalis* | 18 | 15.6 | Santacrucian | Octodontoidea | (3, 22, 38) |
| *Neophanomys biplicatus* | 8.9 | 5.1 | Late Miocene | Octodontoidea | (40, 46) |
| *Pithanotomys columnaris* | 4.7 | 3.7 | Montehermosan | Octodontoidea | (40, 45) |
| *Deseadomys arambourgi* | 29.4 | 24.2 | Deseadan | Octodontoidea | (17, 35) |
| *Adelphomys candidus* | 19.04 | 15.6 | Pinturan-Santacrucian | Octodontoidea | (17, 22, 44, 45) |
| *Prostichomys bowni* | 19.04 | 15.6 | Pinturan-Santacrucian | Octodontoidea | (17, 32, 44) |
| *Stichomys regularis* | 18 | 15.6 | Santacrucian | Octodontoidea | (22, 45) |
| *Maruchito trilofodonte* | 15.7 | 14 | Colloncuran | Octodontoidea | (41, 47) |
| *Pampamys emmonsae* | 8.9 | 5.1 | Late Miocene | Octodontoidea | (40, 48) |
| *Mayomys confluens* | 32.5 | 28.3 | Early Oligocene | Caviomorpha | (16, 49, 50) |
| *Leucokephalos zeffiae* | 29.4 | 24.2 | Deseadan | Octodontoidea | (17, 51) |
| *Chambiramys sylvaticus* | 26.6 | 23.03 | Late Oligocene | Chinchilloidea | (16, 23) |
| *Chambiramys shipiborum* | 26.6 | 23.03 | Late Oligocene | Chinchilloidea | (16, 23) |
| *Borikenomys praecursor* | 29.78 | 29.17 | Early Oligocene | Chinchilloidea | (5) |
| *Elasmodontomys obliquus* | 0.774 | 0.002 | Pleistocene-Holocene | Chinchilloidea | (5, 52, 53) |
| *Amblyrhiza inundata* | 0.5 | 0.079 | Middle-Late Pleistocene | Chinchilloidea | (53–55) |
| *Phoberomys pattersoni* | 11.6 | 5.3 | Late Miocene | Chinchilloidea | (56, 57) |
| *Josephoartigasia monesi* | 4.0 | 2.0 | Pliocene-Pleistocene | Chinchilloidea | (6) |

**Table S5.** Body mass (BM) estimates in grams (gr) of the extinct species of Chinchilloidea and Octodontoidea included in this study. Details of BM estimates obtained in this study are in Table S6.

| Species | BM | BM min | BM max | BM source | Comments |
|---|---|---|---|---|---|
| *Eoincamys pascuali* | 178 | 98 | 257 | This study | |
| *Eoincamys ameghinoi* | 101 | 56 | 145 | This study | |
| *Eoincamys valverdei* | 215 | 119 | 311 | This study | |
| *Eoincamys parvus* | 104 | 58 | 151 | This study | |
| *Incamys bolivianus* | 738 | 409 | 1067 | This study | 417 gr estimated by (58) |
| *Scleromys quadrangulatus* | 2639 | 1462 | 3816 | This study | |
| *Scleromys osbornianus* | 3065 | 1698 | 4431 | This study | |
| *Scleromys angustus* | 6238 | 3456 | 9019 | This study | |
| *Maquiamys praecursor* | | No data | | (23, 45) | Only known from isolated upper teeth |
| *Microscleromys paradoxalis* | 150 | 100 | 200 | (24, 25) | |
| *Microscleromys cribriphilus* | 150 | 100 | 200 | (24, 25) | |
| *Drytomomys aequatorialis* | 9775 | 5415 | 14135 | This study | |
| *Potamarchus murinus* | 16000 | 13000 | 19000 | (59) | |
| *Neoepiblema horridula* | 72400 | 65300 | 79500 | (28, 60–62) | Assuming similar body mass as the sister species *Neoepiblema acreensis* |
| *Garridomys curnunuquem* | 651 | 361 | 941 | This study | |
| *Eoviscaccia frassinetti* | 923 | 511 | 1335 | This study | |
| *Eoviscaccia australis* | 328 | 182 | 475 | This study | |
| *Perimys intermedius* | 1379 | 764 | 1994 | This study | |
| *Draconomys verai* | 268 | 148 | 387 | This study | |
| *Platypittamys brachyodon* | 81 | 45 | 118 | This study | |
| *Eosallamys paulacoutoi* | 534 | 296 | 771 | This study | |
| *Eosallamys simpsoni* | 278 | 154 | 403 | This study | |
| *Sallamys pascuali* | 191 | 106 | 277 | This study | 134 gr estimated by (58) |
| *Prospaniomys priscus* | 577 | 326 | 827 | This study | |
| *Spaniomys riparius* | 549 | 304 | 794 | This study | 649 gr estimated by (58) |
| *Protadelphomys latus* | 508 | 288 | 728 | This study | |
| *Willidewu esteparius* | 234 | 130 | 338 | This study | |
| *Xenodontomys simpsoni* | 384 | 212 | 555 | This study | |
| *Xenodontomys elongatus* | 1318 | 730 | 1906 | This study | |
| *Caviocricetus lucasi* | 145 | 80 | 209 | This study | |
| *Acaremys murinus* | 162 | 90 | 234 | This study | |
| *Plesiacarechimys koenigwaldi* | 640 | 354 | 925 | This study | |
| *Dudumus ruigomezi* | 178 | 98 | 257 | This study | |
| *Galileomys eurygnathus* | 215 | 119 | 311 | This study | |

| | | | | | |
|---|---|---|---|---|---|
| *Sciamys principalis* | 268 | 148 | 387 | This study | |
| *Neophanomys biplicatus* | 93 | 52 | 135 | This study | |
| *Pithanotomys columnaris* | 299 | 166 | 433 | This study | |
| *Deseadomys arambourgi* | 349 | 193 | 504 | This study | |
| *Adelphomys candidus* | | No data | | | No dental measurements available in the literature |
| *Prostichomys bowni* | 379 | 210 | 548 | This study | |
| *Stichomys regularis* | 838 | 464 | 1212 | This study | |
| *Maruchito trilofodonte* | 698 | 386 | 1009 | This study | |
| *Pampamys emmonsae* | 224 | 124 | 324 | This study | |
| *Mayomys confluens* | 112 | 62 | 162 | This study | |
| *Leucokephalos zeffiae* | 162 | 90 | 234 | This study | |
| *Chambiramys sylvaticus* | 175 | 97 | 253 | This study | |
| *Chambiramys shipiborum* | | No data | | (23) | Only known from isolated upper teeth, m3 and dp4 |
| *Borikenomys praecursor* | | No data | | (5) | Only known from isolated m3 |
| *Elasmodontomys obliquus* | 13700 | 9400 | 17600 | (63) | |
| *Amblyrhiza inundata* | 125000 | 50000 | 200000 | (64) | |
| *Phoberomys pattersoni* | 150000 | 62500 | 296000 | (62) | |
| *Josephoartigasia monesi* | 483000 | 224000 | 1041000 | (6, 62) | |

**Table S6.** Dental measurements (in mm) and body mass (BM) estimates (in grams) of extinct species of Chinchilloidea and Octodontoidea. * indicates tooth length of unidentified lower molar(s) in species where isolated m1, m2, or m3 cannot be distinguished based on morphology or size. N = number of specimens. UTRL = upper tooth row length. BM estimates were obtained using the regression equations of (65).

| Species | m1 length | N | UTRL | BM | BM min | BM max | Measure references |
|---|---|---|---|---|---|---|---|
| *Eoincamys pascuali** | 1.91 | 10 | | 178 | 98 | 257 | (14, 49) |
| *Eoincamys ameghinoi** | 1.57 | 12 | | 101 | 56 | 145 | (14, 49) |
| *Eoincamys valverdei** | 2.04 | 8 | | 215 | 119 | 311 | (49) |
| *Eoincamys parvus** | 1.59 | 4 | | 104 | 58 | 151 | (49) |
| *Incamys bolivianus* | 3.12 | 27 | | 738 | 409 | 1067 | (36) |
| *Scleromys quadrangulatus* | 4.84 | 5 | | 2639 | 1462 | 3816 | (20) |
| *Scleromys osbornianus* | 5.10 | 1 | | 3065 | 1698 | 4431 | Estimated from (20 fig 3) |
| *Scleromys angustus** | 6.51 | 1 | | 6238 | 3456 | 9019 | Estimated from (20 fig 3) |
| *Maquiamys praecursor* | | | No data | | | | (23, 45) |
| *Drytomomys aequatorialis* | 7.6 | 1 | | 9775 | 5415 | 14135 | (66) |
| *Garridomys curnunuquem* | 3.0 | 10 | | 651 | 361 | 941 | (29) |
| *Eoviscaccia frassinetti* | 3.37 | 1 | | 923 | 511 | 1335 | (30) |
| *Eoviscaccia australis** | 2.36 | 7 | | 328 | 182 | 475 | (31) |
| *Perimys intermedius* | 3.87 | 25 | | 1379 | 764 | 1994 | (33) |
| *Draconomys verai* | 2.2 | 4 | | 268 | 148 | 387 | (21) |
| *Platypittamys brachyodon* | 1.46 | 1 | | 81 | 45 | 118 | (67) |
| *Eosallamys paulacoutoi** | 2.79 | 3 | | 534 | 296 | 771 | (14) |
| *Eosallamys simpsoni** | 2.23 | 7 | | 278 | 154 | 403 | (14) |
| *Sallamys pascuali* | 1.96 | 6 | | 191 | 106 | 277 | (36) |
| *Prospaniomys priscus* | | 1 | 10.9 | 577 | 326 | 827 | (37) |
| *Spaniomys riparius* | 2.82 | | | 549 | 304 | 794 | m1 length estimated from (68 fig 2) |
| *Protadelphomys latus* | | 1 | 10.1 | 508 | 288 | 728 | (69, 70) |
| *Willidewu esteparius* | 2.10 | 1 | | 234 | 130 | 338 | (71) |
| *Xenodontomys simpsoni* | 2.49 | 7 | | 384 | 212 | 555 | (39) |
| *Xenodontomys elongatus* | 3.81 | 84 | | 1318 | 730 | 1906 | (39) |
| *Caviocricetus lucasi* | 1.78 | 19 | | 145 | 80 | 209 | (72) |
| *Acaremys murinus* | 1.85 | 2 | | 162 | 90 | 234 | (4) |
| *Plesiacarechimys koenigwaldi* | 2.97 | 6 | | 640 | 354 | 925 | (73) |
| *Dudumus ruigomezi* | 1.91 | 6 | | 178 | 98 | 257 | (43) |
| *Galileomys eurygnathus* | 2.04 | 8 | | 215 | 119 | 311 | (44) |
| *Sciamys principalis* | 2.20 | 1 | | 268 | 148 | 387 | (3) |
| *Neophanomys biplicatus* | 1.53 | 3 | | 93 | 52 | 135 | (46) |
| *Pithanotomys columnaris* | 2.29 | 1 | | 299 | 166 | 433 | m1 length estimated from (74) |
| *Deseadomys arambourgi* | 2.41 | 1 | | 349 | 193 | 504 | (35) |

| | | | | | | |
|---|---|---|---|---|---|---|
| *Adelphomys candidus* | | | No data | | | |
| *Prostichomys bowni* | 2.48 | 6 | 379 | 210 | 548 | (75) |
| *Stichomys regularis* | 3.26 | 1 | 838 | 464 | 1212 | (3) |
| *Maruchito trilofodonte* | 3.06 | 3 | 698 | 386 | 1009 | (47) |
| *Pampamys emmonsae* | 2.07 | 12 | 224 | 124 | 324 | (76) |
| *Mayomys confluens* | 1.63 | 29 | 112 | 62 | 162 | (49) |
| *Leucokephalos zeffiae* | 1.85 | 4 | 162 | 90 | 234 | (51) |
| *Chambiramys sylvaticus* | 1.90 | 1 | 175 | 97 | 253 | (23) |
| *Chambiramys shipiborum* | | | No data | | | (23) |
| *Borikenomys praecursor* | | | No data | | | (5) |

**Craniodental traits of extant species – Dataset S1.** Craniodental measurements of extant species of Chinchilloidea and Octodontoidea. Measurements abbreviations correspond to Figure 3 and Table S1. Values in milimeters (mm). IDAS = individual dental ages (77); NA = measurement could not be taken.

**Body mass and cranial traits in extinct and extant species – Dataset S2.** Body mass of extant and extinct Chinchilloidea and Octodontoidea (Table S5 and S6) and average values per species of the craniodental measurements of extant species. Measurements abbreviations correspond to Figure 3 and Table S1. Values in milimeters (mm).

**Time calibrated phylogenetic analysis of extinct and extant Chinchilloidea and Octodontoidea – Dataset S3.** This dataset includes the nexus and xml files with the molecular and morphological data used in the phylogenetic analyses. It also includes the annotated python script to concatenated the mitochondrial and nuclear molecular data, and the annotated R scripts to estimate the age of origin of Chinchilloidea + Octodontoidea using he Bayesian Brownian bridge (BBB) model (78).

**Analyses of body mass evolution in Chinchilloidea and Octodontoidea – Dataset S4.** This dataset includes the input and output files used in the Bayesian analyses of body mass evolution. It includes the obtained post-burning trees and files and code used in the fossilBM program (79, 80). It also includes the annotated R scripts to obtain and plot the rates of body mass evolution for both clades.

**Lineage through time diversity of Chinchilloidea and Octodontoidea – Dataset S5.** This dataset includes the trees and annotated R script using to obtain the lineage through time (LLT) diversity of Chinchilloidea and Octodontoidea.

**Diversfication rates of Chinchilloidea and Octodontoidea – Dataset S6.** This dataset includes the files and annotated R script to estimate the diversification rates of Chinchilloidea and Octodontoidea using the Fossilized Birth-Death (FBD) skyline model (81, 82) as implemented in BEAST2 v.2.6.7 (83) and following (84).

**Morphospace occupation of extant Chinchilloidea and Octodontoidea – Dataset S7.** This dataset includes the files and annotated R script to estimate the phylomorphospace of extant Chinchilloidea and Octodontoidea and compare their morphospace occupation considering the differences in species richness.

## SI References


1. D. Edler, J. Klein, A. Antonelli, D. Silvestro, raxmlGUI 2.0: A graphical interface and toolkit for phylogenetic analyses using RAxML. *Methods in Ecology and Evolution* **12**, 373–377 (2021).

2. N. S. Upham, B. D. Patterson, "Evolution of caviomorph rodents: a complete phylogeny and timetree for living genera" in *Biology of Caviomorph Rodents: Diversity and Evolution*, A. I. Vasallo, D. Antenucci, Eds. (SAREM- Sociedad Argentina para el Estudio de los Mamíferos, 2015), pp. 63–120.

3. M. Arnal, M. E. Pérez, A new acaremyid rodent (Hystricognathi: Octodontoidea) from the middle Miocene of Patagonia (South America) and considerations on the early evolution of Octodontoidea. *Zootaxa* **3616**, 119–134 (2013).

4. M. Arnal, M. G. Vucetich, Revision of the fossil rodent *Acaremys* Ameghino, 1887 (Hystricognathi, Octodontoidea, Acaremyidae) from the Miocene of Patagonia (Argentina) and the description of a new acaremyid. *Historical Biology* **27**, 42–59 (2015).

5. L. Marivaux, *et al.*, Early Oligocene chinchilloid caviomorphs from Puerto Rico and the initial rodent colonization of the West Indies. *Proceedings of the Royal Society B* **287**, 20192806 (2020).

6. A. Rinderknecht, R. E. Blanco, The largest fossil rodent. *Proceedings of the Royal Society B: Biological Sciences* **275**, 923–928 (2008).

7. L. L. Rasia, A. M. Candela, C. Cañón, Comprehensive total evidence phylogeny of chinchillids (Rodentia, Caviomorpha): Cheek teeth anatomy and evolution. *Journal of Anatomy* **239**, 405–423 (2021).

8. D. Verzi, A. I. Olivares, C. C. Morgan, Phylogeny and evolutionary patterns of South American Octodontoid rodents. *Acta Palaeontologica Polonica* **59**, 757–769 (2013).

9. M. Gendre, T. Hauffe, C. Pimiento, D. Silvestro, Benchmarking imputation methods for discrete biological data. 2023.04.06.535892 (2023).

10. L. A. B. Wilson, Allometric disparity in rodent evolution. *Ecology and Evolution* **3**, 971–984 (2013).

11. W. C. Tavares, L. M. Pessôa, H. N. Seuánez, Phylogenetic and size constrains on cranial ontogenetic allometry of spiny rats (Echimyidae, Rodentia). *Journal of Evolutionary Biology* **29**, 1752–1765 (2016).

12. W. C. Tavares, L. M. Pessôa, H. N. Seuánez, Changes in ontogenetic allometry and their role in the emergence of cranial morphology in fossorial spiny rats (Echimyidae, Hystricomorpha, Rodentia). *Journal of Mammalian Evolution*, 1–11 (2018).

13. R. Lanfear, P. B. Frandsen, A. M. Wright, T. Senfeld, B. Calcott, PartitionFinder 2: new methods for selecting partitioned models of evolution for molecular and morphological phylogenetic analyses. *Molecular Biology and Evolution* **34**, 772–773 (2017).

14. C. D. Frailey, K. E. Campbell, "Paleogene Rodents from Amazonian Peru: The Santa Rosa Local Fauna" in *The Paleogene Mammalian Fauna of Santa Rosa, Amazonian Peru*, (Natural History Museum of Los Angeles County, 2004), pp. 71–130.

15. E. R. Seiffert, *et al.*, A parapithecid stem anthropoid of African origin in the Paleogene of South America. *Science* **368**, 194–197 (2020).

16. K. E. Campbell, P. B. O'Sullivan, J. G. Fleagle, D. de Vries, E. R. Seiffert, An Early Oligocene age for the oldest known monkeys and rodents of South America. *Proc Natl Acad Sci USA* **118**, e2105956118 (2021).

17. R. E. Dunn, *et al.*, A new chronology for middle Eocene-early Miocene South American Land Mammal Ages. *Bulletin of the Geological Society of America* **125**, 539–555 (2013).

18. F. Busker, M. T. Dozo, First confirmed record of *Incamys bolivianus* (Caviomorpha, Chinchilloidea) in the Deseadan of Patagonia (Argentina). *ameg* **54**, 706–712 (2017).

19. A. M. Candela, M. E. Pérez, L. L. Rasia, E. Cerdeño, New late Oligocene caviomorph rodents from Mendoza province, central-western Argentina. *vrpa* **41** (2021).

20. A. G. Kramarz, *Neoreomys* and *Scleromys* (Rodentia, Hystricognathi) from the Pinturas Formation, late Early Miocene of Patagonia, Argentina. *Rev. Mus. Argentino Cienc. Nat.* **8**, 53–62 (2006).

21. A. G. Kramarz, *et al.*, "A New Mammal Fauna at the Top of the Gran Barranca Sequence and its Biochronological Significance" in *The Paleontology of Gran Barranca. Evolution and*

*Environmental Change through the Middle Cenozoic of Patagonia*, R. H. Madden, A. A. Carlini, M. G. Vucetich, R. F. Kay, Eds. (Cambridge University Press, 2010), pp. 264–277.

22. J. I. Cuitiño, *et al.*, U-Pb geochronology of the Santa Cruz Formation (early Miocene) at the Río Bote and Río Santa Cruz (southernmost Patagonia, Argentina): Implications for the correlation of fossil vertebrate localities. *Journal of South American Earth Sciences* **70**, 198–210 (2016).

23. M. Boivin, *et al.*, Late Oligocene caviomorph rodents from Contamana, Peruvian Amazonia. *Papers in Palaeontology* **3**, 69–109 (2017).

24. A. H. Walton, "Rodents of the La Venta Fauna, Miocene, Colombia: Biostratigraphy and Paleoenvironmental implications," Southern Methodist University. (1990).

25. A. H. Walton, "Rodents" in *Vertebrate Paleontology in the Neotropics. The Miocene Fauna of La Venta*, R. F. Kay, R. H. Madden, R. L. Cifelli, J. J. Flynn, Eds. (Smithsonian Institution Press, 1997), pp. 392–409.

26. A. Candela, N. L. Nasif, Systematics and biogeographic significance of *Drytomomys typicus* (Scalabrini in Ameghino, 1889 ) nov. comb., a Miocene Dinomyidae (Rodentia, Hystricognathi) from northeast of Argenitna. *Neues Jahrbuch für Geologie und Paläontologie, Abhandlungen* **3**, 165–181 (2006).

27. L. Kerber, F. Negri, A. Ribeiro, M. Vucetich, J. Souza Filho, Late Miocene potamarchine rodents (Caviomorpha: Dinomyidae) from southwestern Amazonia, Brazil (northern South America): with description of new taxa. *Acta Palaeontologica Polonica* **61**, 191–203 (2016).

28. L. Kerber, F. R. Negri, D. Sanfelice, Morphology of cheek teeth and dental replacement in the extinct rodent *Neoepiblema* Ameghino, 1889 (Caviomorpha, Chinchilloidea, Neoepiblemidae). *Journal of Vertebrate Paleontology* **38**, e1549061 (2019).

29. A. G. Kramarz, M. G. Vucetich, M. Arnal, A new early Miocene chinchilloid hystricognath rodent; an approach to the understanding of the early chinchillid dental evolution. *Journal of Mammalian Evolution* **20**, 249–261 (2013).

30. O. C. Bertrand, J. J. Flynn, D. A. Croft, A. R. Wyss, Two new taxa (Caviomorpha, Rodentia) from the early Oligocene Tinguiririca fauna (Chile). *novi* **2012**, 1–36 (2012).

31. A. G. Kramarz, Registro de *Eoviscaccia* (Rodentia, Chinchillidae) en estratos colhuehuapenses de Patagonia, Argentina. *Ameghiniana* **38**, 237–242 (2001).

32. M. G. Vucetich, A. G. Kramarz, A. M. Candela, "Colhuehuapian rodents fron Gran Barranca and other Patagonian localities: state of the art" in *The Paleontology of Gran Barranca. Evolution and Environmental Change through the Middle Cenozoic of Patagonia*, (Cambridge University Press, 2010), pp. 206–219.

33. A. Kramarz, Roedores chinchilloideos (Hystricognathi) de la Formación Pinturas, Mioceno temprano-medio de la provincia de Santa Cruz, Argentina. *Revista del Museo Argentino de Ciencias Naturales nueva serie* **4**, 167–180 (2002).

34. M. G. Vucetich, E. C. Vieytes, M. E. Pérez, A. A. Carlini, "The rodents from La Cantera and the early evolution of caviomorphs in South America" in *The Paleontology of Gran Barranca. Evolution and Environmental Change through the Middle Cenozoic of Patagonia*, (Cambridge University Press, 2010).

35. A. E. Wood, B. Patterson, The rodents of the Deseadan Oligocene of Patagonia and the beginnings of South American rodent evolution, by Albert E. Wood and Bryan Patterson. *Bulletin of the Museum of Comparative Zoology at Harvard College.* **120**, 279–428 (1959).

36. B. Patterson, A. E. Wood, Rodents from the Deseadan Oligocene of Bolivia and the relationships of the caviomorpha. *Bulletin of the Museum of Comparative Zoology at Harvard College.* **149**, 371–543 (1982).

37. M. Arnal, A. G. Kramarz, First complete skull of an octodontoid (Rodentia, Caviomorpha) from the Early Miocene of South America and its bearing in the early evolution of Octodontoidea. *Geobios* **44**, 435–444 (2011).

38. J. J. Flynn, *et al.*, A new fossil mammal assemblage from the southern Chilean Andes: implications for geology, geochronology, and tectonics. *Journal of South American Earth Sciences* **15**, 285–302 (2002).

39. D. H. Verzi, C. I. Montalvo, S. I. Tiranti, Un nuevo *Xenodontomys* (Rodentia, Octodontidae) del Mioceno tardío de La Pampa, Argentina. Patrón evolutivo y biocronología. *Ameghiniana* **40**, 229–238 (2003).

40. F. J. Prevosti, *et al.*, New radiometric 40Ar–39Ar dates and faunistic analyses refine evolutionary dynamics of Neogene vertebrate assemblages in southern South America. *Scientific Reports* **11**, 9830 (2021).

41. R. H. Madden, *et al.*, "The Laventan Stage and Age" in *Vertebrate Paleontology in the Neotropics. The Miocene Fauna of La Venta, Colombia*, R. F. Kay, R. H. Madden, R. L. Cifelli, J. J. Flynn, Eds. (Smithsonian Institution Press, 1997), pp. 355–381.

42. M. G. Vucetich, E. C. Vieytes, A Middle Miocene primitive octodontoid rodent and its bearing on the early evolutionary history of the Octodontoidea. *Palaeontographica Abteilung A*, 81–91 (2006).

43. M. Arnal, A. G. Kramarz, M. G. Vucetich, E. C. Vieytes, A new early Miocene octodontoid rodent (Hystricognathi, Caviomorpha) from Patagonia (Argentina) and a reassessment of the early evolution of Octodontoidea. *Journal of Vertebrate Paleontology* **34**, 397–406 (2014).

44. A. G. Kramarz, Octodontoids and erethizontoids (Rodentia, Hystricognathi) from the Pinturas Formation, Early - Middle Miocene of Patagonia, Argentina. *Ameghiniana* **41**, 199–216 (2004).

45. M. Boivin, L. Marivaux, P.-O. Antoine, L'apport du registre paléogène d'Amazonie sur la diversification initiale des Caviomorpha (Hystricognathi, Rodentia) : implications phylogénétiques, macroévolutives et paléobiogéographiques. *Geodiversitas* **41**, 143–245 (2019).

46. D. H. Verzi, E. C. Vieytes, C. I. Montalvo, Dental evolution in *Neophanomys* (Rodentia, Octodontidae) from the late Miocene of central Argentina. *Geobios* **44**, 621–633 (2011).

47. M. G. Vucetich, M. M. Mazzoni, U. F. J. Pardiñas, Los roedores de la Formación Collon Cura (Mioceno Medio), y la ignimbrita Pilcaniyeu. Canadon del Tordillo, Neuquen. *Ameghiniana* **30**, 361–381 (1993).

48. A. I. Olivares, D. H. Verzi, M. G. Vucetich, C. I. Montalvo, Phylogenetic affinities of the late Miocene echimyid *† Pampamys* and the age of *Thrichomys* (Rodentia, Hystricognathi). *Journal of Mammalogy* **93**, 76–86 (2012).

49. M. Boivin, *et al.*, Early Oligocene caviomorph rodents from Shapaja, Peruvian Amazonia. *Palaeontographica Abteilung A*, 87–156 (2018).

50. P.-O. Antoine, *et al.*, Biotic community and landscape changes around the Eocene–Oligocene transition at Shapaja, Peruvian Amazonia: Regional or global drivers? *Global and Planetary Change* **202**, 103512 (2021).

51. M. G. Vucetich, M. T. Dozo, M. Arnal, M. E. Pérez, New rodents (Mammalia) from the late Oligocene of Cabeza Blanca (Chubut) and the first rodent radiation in Patagonia. *Historical Biology* **27**, 236–257 (2015).

52. S. t Turvey, J. r Oliver, Y. m Narganes Storde, P. Rye, Late Holocene extinction of Puerto Rican native land mammals. *Biology Letters* **3**, 193–196 (2007).

53. R. D. E. MacPhee, Basicranial morphology and relationships of antillean Heptaxodontidae (Rodentia, Ctenohystrica, Caviomorpha). *Bulletin of the American Museum of Natural History* **363**, 1–70 (2011).

54. D. A. McFarlane, R. D. E. MacPhee, D. C. Ford, Body size variability and a Sangamonian extinction model for *Amblyrhiza*, a West Indian megafaunal rodent. *Quat. res.* **50**, 80–89 (1998).

55. D. A. McFarlane, J. Lundberg, G. Maincent, New specimens of *Amblyrhiza inundata* (Rodentia: Caviomorpha) from the Middle Pleistocene of Saint Barthélemy, French West Indies. *Caribbean Journal of Earth Science* **47**, 15–19 (2014).

56. L. I. Quiroz, C. A. Jaramillo, "Stratigraphy and sedimentary environments of Miocene shallow to marginal marine deposits in the Urumaco trough, Falcón basin, western Venezuela" in *Urumaco & Venezuelan Paleontology. The Fossil Record of the Northern Neotropics*, M. R. Sánchez-Villagra, O. A. Aguilera, A. A. Carlini, Eds. (Indiana University Press, 2010), pp. 153–172.

57. J. D. Carrillo, M. R. Sánchez-Villagra, Giant rodents from the Neotropics: diversity and dental variation of late Miocene neoepiblemid remains from Urumaco, Venezuela. *Palaontologische Zeitschrift* **89**, 1057–1071 (2015).

58. D. A. Croft, "Archaeohyracidae (Mammalia: Notoungulata) from the Tinguiririca Fauna, central Chile, and the evolution and paleoecology of South American mammalian herbivores," Ann Arbor, United States. (2000) (October 11, 2022).

59. M. G. Vucetich, M. Arnal, C. M. Deschamps, M. E. Perez, E. C. Vieytes, "A Brief History of Caviomorph Rodents as Told by the Fossil Record" in *Biology of Caviomorph Rodents: Diversity and Evolution*, A. I. Vassallo, D. Antenucci, Eds. (SAREM- Sociedad Argentina para el Estudio de los Mamíferos, 2015), pp. 11–62.

60. L. Kerber, *et al.*, Postcranial morphology of the extinct rodent *Neoepiblema* (Rodentia: Chinchilloidea): insights into the paleobiology of neoepiblemids. *J Mammal Evol* **29**, 207–235 (2022).

61. J. D. Ferreira, F. R. Negri, M. R. Sánchez-Villagra, L. Kerber, Small within the largest: brain size and anatomy of the extinct *Neoepiblema acreensis*, a giant rodent from the Neotropics. *Biology Letters* **16**, 20190914 (2020).

62. R. K. Engelman, Resizing the largest known extinct rodents (Caviomorpha: Dinomyidae, Neoepiblemidae) using occipital condyle width. *R. Soc. open sci.* **9**, 220370 (2022).

63. D. A. McFarlane, Late Quaternary fossil mammals and last occurrence dates from Caves at Barahona, Puerto Rico. *Caribbean Journal of Science* **35**, 238–248 (1999).

64. A. R. Biknevicius, D. a. McFarlane, R. D. E. Macphee, Body size in *Amblyrhiza inundata* (Rodentia: Caviomorpha), an extinct megafaunal rodent from the Anguilla Bank, West Indies: estimates and implications. *American Museum Novitates* **3079**, 1–25 (1993).

65. V. Millien, H. Bovy, When teeth and bones disagree: body mass estimation of a giant extinct rodent. *Journal of Mammalogy* **91**, 11–18 (2010).

66. R. W. Fields, Hystricomorph rodents from the late Miocene of Colombia, South America. *University of California Publications in Geological Sciences* **32**, 273–404 (1957).

67. A. E. Wood, A new Oligocene rodent genus from Patagonia. *Oligocene rodent from Patagonia* **1435** (1949).

68. D. K. Anderson, J. Damuth, T. M. Bown, Rapid morphological change in Miocene marsupials and rodents associated with a volcanic catastrophe in Argentina. *Journal of Vertebrate Paleontology* **15**, 640–649 (1995).

69. M. G. Vucetich, M. Bond, Un nuevo Octodontoidea (Rodentia, Caviomorpha) del Oligoceno tardío de la Provincia de Chubut (Argentina). *Ameghiniana* **21**, 104–114 (1984).

70. M. G. Vucetich, D. H. Verzi, M. T. Dozo, El "status" sistemático de *Gaimanomys alwinea* (Rodentia, Caviomorpha, Echimyidae). *Ameghiniana* **29**, 85–86 (1992).

71. M. G. Vucetich, D. H. Verzi, Un nuevo Echimyidae (Rodentia, Hystricognathi) de la edad Colhuehapense de Patagonia y consideraciones sobre la sistemática de la familia. *Ameghiniana* **28**, 67–74 (1991).

72. M. G. Vucetich, D. H. Verzi, A peculiar octodontoid (Rodentia, Caviomorpha) with terraced molars from the lower Miocene of Patagonia (Argentina). *Journal of Vertebrate Paleontology* **16**, 297–302 (1996).

73. M. G. Vucetich, E. C. Vieytes, A Middle Miocene primitive octodontoid rodent and its bearing on the early evolutionary history of the Octodontoidea. *pala* **277**, 81–91 (2006).

74. C. M. Deschamps, M. G. Vucetich, D. H. Verzi, A. I. Olivares, Biostratigraphy and correlation of the Monte Hermoso Formation (early Pliocene, Argentina): The evidence from caviomorph rodents. *Journal of South American Earth Sciences* **35**, 1–9 (2012).

75. A. G. Kramarz, Un nuevo roedor Adelphomyinae (Hystricognathi, Echimyidae) del Mioceno Medio-Inferior de Patagonia, Argentina. *Ameghiniana* **38**, 163–168 (2001).

76. D. H. Verzi, M. G. Vucetich, C. I. Montalvo, Un nuevo Eumysopinae (Rodentia, Echimyidae) del Mioceno tardio de la provincia de La Pampa y consideraciones sobre la historia de la subfamilia. *Ameghiniana* **32**, 191–195 (1995).

77. U. Anders, W. von Koenigswald, I. Ruf, B. H. Smith, Generalized individual dental age stages for fossil and extant placental mammals. *Palaontologische Zeitschrift* **85**, 321–339 (2011).

78. D. Silvestro, *et al.*, Fossil data support a pre-Cretaceous origin of flowering plants. *Nature Ecology & Evolution 2021 5:4* **5**, 449–457 (2021).

79. D. Silvestro, *et al.*, Early arrival and climatically-linked geographic expansion of New World monkeys from tiny African ancestors. *Systematic Biology* (2018) https:/doi.org/10.1093/sysbio/syy046.

80. Q. Zhang, R. H. Ree, N. Salamin, Y. Xing, D. Silvestro, Fossil-Informed Models Reveal a Boreotropical Origin and Divergent Evolutionary Trajectories in the Walnut Family (Juglandaceae). *Systematic Biology* **71**, 242–258 (2022).

81. T. Stadler, D. Kühnert, S. Bonhoeffer, A. J. Drummond, Birth–death skyline plot reveals temporal changes of epidemic spread in HIV and hepatitis C virus (HCV). *Proceedings of the National Academy of Sciences* **110**, 228–233 (2013).

82. A. Gavryushkina, D. Welch, T. Stadler, A. J. Drummond, Bayesian inference of sampled ancestor trees for epidemiology and fossil calibration. *PLOS Computational Biology* **10**, e1003919 (2014).

83. R. Bouckaert, *et al.*, BEAST 2.5: An advanced software platform for Bayesian evolutionary analysis. *PLOS Computational Biology* **15**, e1006650 (2019).

84. B. Allen, M. V. Volkova, T. Stadler, T. G. Vaughan, R. C. Warnock, Mechanistic phylodynamic models do not provide conclusive evidence that non-avian dinosaurs were in decline before their final extinction. *Cambridge Prisms: Extinction* (In press).